ORNL-4118

Contract No. W-7405-eng-26

Neutron Physics Division

ESTABLISHING AN ENERGY SCALE FOR PULSE-HEIGHT DISTRIBUTIONS FROM GAMMA-RAY SPECTROMETERS BASED ON INORGANIC SCINTILLATORS

R. W. Peelle and T. A. Love

NOTE:

This Work Partially Supported by
NATIONAL AERONAUTICS AND SPACE ADMINISTRATION
Under Order R-104(1)

OCTOBER 1967

OAK RIDGE NATIONAL LABORATORY
Oak Ridge, Tennessee
operated by
UNION CARBIDE CORPORATION
for the
U.S. ATOMIC ENERGY COMMISSION

CONTENTS

PREFACE

This report on the problems associated with calibration of scintillation gamma-ray spectrometers was completed in the fall of 1965 as a chapter for a multi-author review book on the scintillation spectroscopy of gamma radiation. Publication of this book has been delayed, so the isolated chapter is offered here after minor revision.

The text is directed at the beginner in scintillation spectrometry who has a general knowledge of the physics and technology of scintillation counting. The necessary background and coordinate information may be found in earlier works such as those listed below:

(a) G. D. O'Kelley, "Gamma-Ray Scintillation Spectrometry," pp 616-641 in Methods of Experimental Physics, Vol. 5, Part A, edited by Luke C. L. Yuan and Chien-Shiung Wu, Academic Press (1961).

(b) R. B. Murray, "Scintillation Counters," pp 82-165 in Nuclear Instruments and Their Uses, edited by A. H. Snell, Wiley (1962).

(c) J. B. Birks, The Theory and Practice of Scintillation Counting, MacMillan, New York (1964) Chaps. 4, 5, 11, 12, and 16.

(d) J. H. Neiler and P. R. Bell, "The Scintillation Method," pp 245-302 in α-β-γ-Ray Spectroscopy, edited by Kai Siegbahn, North Holland Publishing Co. (1965).

ESTABLISHING AN ENERGY SCALE FOR PULSE-HEIGHT DISTRIBUTIONS FROM GAMMA-RAY SPECTROMETERS BASED ON INORGANIC SCINTILLATORS

R. W. Peelle and T. A. Love

ABSTRACT

Devices, experiment designs, and data analysis techniques useful for the calibration of scintillation gamma-ray spectrometers are critically examined. Though the ideas have broader application, the discussion assumes the use of NaI(Tl) phosphors. The review of calibration sources includes tables of gamma-emitting radioisotopes employable for this purpose, with best energies, uncertainties, and other convenient data. The branching ratios among the naturally mixed x-ray lines (K-L vs K-M + K-N) are tabulated for useful radioisotope x-ray sources to enable use of a simple method given for determining the appropriate "effective" energy of the mixed source. The origins of spectrometer instability and nonlinearity are reviewed along with their relative importances, and defensive experiment designs and data analysis techniques are discussed. For finding the central position of the peak in a pulse-height distribution from gamma rays of a single energy, all the standard numerical and graphical methods are illustrated and compared, including full and partial nonlinear least-squares analyses. Finally, interpolation methods are detailed for determining from the available calibration information an unknown gamma-ray energy and its uncertainty.

I. INTRODUCTION

The energies of gamma rays may be determined using scintillation spectrometers based on phosphors by employing the techniques discussed in this report. Gamma-ray scintillation spectrometry is relative spectrometry, since it is impossible to determine the absolute relation between energy absorbed in a scintillator and the resulting quantity of emitted light without the use of a source which emits gamma-rays of known energy. The scintillation spectroscopist relates unknown gamma-ray energies to known ones by observing accumulated pulse-height frequency functions representing sequences of light flashes produced when a scintillator is exposed to sources of these gamma rays. The gamma-ray energy scale is based on magnetic and crystal diffraction spectrometry.

A series of gamma rays of energy E(MeV) produces by means of a scintillation spectrometer a recorded distribution of pulse heights N(p) (counts per pulse-height channel of unmeasured but stable width). Each observed pulse amplitude p is related statistically to an energy-absorption event in the scintillator. N(p) for a source of monoenergetic gamma rays typically includes a nearly normal distribution of pulse heights corresponding to absorption in the scintillator of the full energy E, as well as a distribution of smaller pulses. We call the mean of the normal distribution P no matter how it has been determined. The function P(E), sampled by determining P_i from $N_i(p)$ for each of a series of source energies E_i, has long been known to approximate a straight line through the origin over the range of gamm-ray energies readily available from radioactive sources.

A beginning spectroscopist using quite standard equipment can measure the energy of a monoenergetic gamma-ray source within 1 or 2% on the first try. Using a few radioactive gamma-ray sources usually to be found around every nuclear laboratory, he can obtain calibration pulse-height spectra which represent the energy-loss distributions in the scintillator. If the apparent pulse-height position of the center of each full-energy peak is plotted against the energy listed for that source in a standard reference work and if not too many points are plotted, a straight line can usually be laid within a reasonable distance of all points. The

full-energy peak of the unknown yields the desired energy upon examination of the plotted line, with an uncertainty which might be suggested by repeating the whole process with a few extra calibration points. Why do such first efforts seem not to give error estimates as small as those claimed by experienced spectroscopists in the literature? How well can extensions of the above process be carried out? This report attacks such questions.

Experienced workers sometimes quote gamma-ray energy determinations by scintillation spectrometry to claimed standard deviations of 0.1%. Such precision is remarkable because this uncertainty may be only 1 or 2% of the width of the full energy peak in the unknown's pulse-height distribution. One can almost promise that sufficiently careful work will result in plausible error estimates no greater than 0.4% in energy over a wide energy region from perhaps 100 keV to 4 MeV, if reasonable statistical accuracy is possible and the unknown "line" is reasonably isolated.

Both expert and novice find that the major attention in reducing experimental uncertainty must be directed toward obtaining reliable and fully understood pulse-height distributions from gamma rays of both standard and unknown energies. Problems of stability in the observed pulse-height distributions are followed closely in importance by questions concerning the linearity of the obtained P(E) vs E "calibration curve." Even the choice of suitable standard energies on which to base interpolation is fraught with uncertainty since too few usable gamma rays have energies known beyond question to uncertainties smaller than 0.05%

The design of appropriate experimental and analytical methods depends upon the required accuracy, the nature and energy range of the unknown gamma-ray spectrum, the availability of proper calibration sources and spectrometer instruments, and perhaps the existence of special environmental difficulties such as high background rates or fluctuations in ambient temperature or magnetic field.

The purpose here is to aid the inexperienced spectroscopist who has determined that his needs are not met by elementary techniques. We discuss the major difficulties which inhibit precise results and how

each may be mitigated, though experimenters readily conquer most of them as soon as their origins are recognized. An attempt is made to assess test and data analysis methods for adequacy and difficulty. Similar questions have been attacked by Julke et al. and Heath et al. (Ju62, He65).

While all references here are to the use of NaI(Tl) scintillators, nearly all the ideas are applicable to CsI(Tl) and many are applicable to lithium-drifted germanium spectrometry.

II. GAMMA-RAY SOURCES FOR ENERGY CALIBRATION

Since the scintillation spectrometrist measures relative energies, he continually requires convenient gamma-ray sources of known energy, where "convenient" and "known" are defined for a particular experiment. When calibration sources must be mounted to preserve the geometry used for measurements of an unknown source, use of otherwise appropriate calibrations may be precluded.

The tables in Sects. B and C below list the transitions which have proved useful. Some lines which have well-determined energy have been omitted because they are not isolated from their neighbors, because they are too weak, or because the material has an inconvenient decay period.

A. Nuclear Reaction Sources

Reaction calibration standards are convenient when the spectrum under investigation is produced in a similar reaction. Nordhagen (No61) lists a series of gamma rays from proton capture, and Jarczyk (Ja61) compares such sources with those neutron capture gamma rays between 3.5 and 10.8 MeV which are readily obtained by pile neutron capture. In these cases the energy precision is not given. Robinson et al. (Ro65) list a series of gamma-ray energies observed through Coulomb excitation.

Most of the gamma-emitting levels in light nuclei may be reached by a variety of reactions, and the level properties are tabulated from time to time (Aj59). The most commonly used levels seem to be the 6.1- and 7.1-MeV levels in ^{16}O reached by the $^{19}F(p,\alpha)$ reaction, and the

4.43-MeV level in ^{12}C reached by inelastic scattering and the $^{11}B(p,\gamma)$ and $^{9}Be(\alpha,n)$ reactions, the last often with natural alpha emitters.

B. Radioisotope Gamma-Ray Sources

Table 1 gives the important properties of pertinent radioisotope gamma-ray emitters. The listed energy values are heavily influenced by the precision magnetic spectrometer work of Murray, Graham, and Geiger (Mu65) and by the germanium detector values of Robinson et al. (Ro65). It is a tribute to the careful error estimates by earlier workers that the new values do not too frequently conflict with the old. In some cases insufficient information was given in the older work to allow correction for minor changes in calibration lines or fundamental constants. A number of the energies have been measured only once with care; others are not so precise as required.* The miscellaneous information included about each emitter is largely from the Nuclear Data Sheets (Nu65) but it is not intended to be definitive or adequately accurate for intensity calibrations.

C. Radioisotope X-Ray Sources

The question of x-ray energies is considerably more complex than that of gamma-ray energies because the undiffracted spectrum of x rays following electron capture or internal conversion is composed of several monoenergetic lines of noticeably different energy. Yet the spectrometrist may need to calibrate in the region below 100 keV, where x-ray sources are plentiful but isolated monoenergetic gamma rays are relatively rare. Use of appropriate x-ray diffraction apparatus can resolve this dilemma.

As examples, consider the relative abundances of the x rays resulting directly from a K-shell vacancy in ^{109}Ag and in ^{203}Tl, given in Table 2. Compared with typical scintillation spectrometry resolutions of 7 and 12 keV, the energies of the components range over 3 and 11 keV, respectively. Since the combined relative abundance of the higher energy K_β

*It seems that the prominent gamma rays from the following isotopes should be measured or remeasured to relative accuracy better than 10^{-3}: ^{7}Be, ^{54}Mn, ^{51}Cr. ^{85}Sr, ^{95}Nb, ^{123m}Te, ^{113}Sn, ^{114}In, and ^{46}Sc.

Table I. Properties of Gamma Rays from Available Radioactive Sources Which Are Useful for Spectrometer Calibration. Only energies are given with precision, averaged from the listed references. If one published value has by far the highest quoted precision, only that value was listed unless it disagreed with earlier work. Minor corrections have been made in some values corresponding to changes in the best values of physical constants. References starting with NRC-... are to the Nuclear Data Sheet (Nu65) so numbered, a type of reference employed when a number of values were considered. For these the uncertainty was based largely on the consistency of the various values. The uncertainties below are estimated standard errors if they have been averaged; otherwise they are the uncertainty quoted in the source. All the well-known prominent gamma rays in each nuclide have been listed together, listed in the order of decreasing energy for the most energetic transition.

Gamma-Ray Energy (keV)	Parent Nuclide	References	Parent Half-Life	Nuclide of Transition	Gamma Rays per Disintegration	Production Method
6135[a] ± 10	^{16}N	Aj59	7.4s	^{16}O	0.7	^{16}O(n,p)
2753.9 ± 0.1 1368.53 ± 0.05	^{24}Na	Mu65	15h	^{24}Mg	1 1	^{23}Na(n,γ) ^{27}Al(n,α)
2614.5 ± 0.1	ThC″ (^{208}Tl)	Mu65	6.7y (^{228}Ra)	^{208}Pb	1	Chemistry
1836.2 ± 0.3 898 ± 0.3	^{88}Y	Ro65 Ba63,Mo61,Ro65	105d	^{88}Sr	1 0.9	^{88}Sr(p,n)
1597[c] ± 2	^{140}Ba(^{140}La)	He52[d]	13d	^{140}Ce	0.9	Fission
1332.48 ± 0.05 1173.23 ± 0.04	^{60}Co	Mu65	5.3y	^{60}Ni	1 1	^{59}Co(n,γ)
1274.6 ± 0.3	^{22}Na	Ro65	2.6y	^{22}Ne	1	^{19}F(α,n) ^{24}Mg(d,α)
1119.3 ± 0.6 888.4 ± 0.4	^{46}Sc	Ba63[d]	85d	^{46}Ti	1 1	^{45}Sc(n,γ)
1115.6 ± 0.3	^{65}Zn	Ro63a,Ro65	245d	^{65}Cu	0.5	^{64}Zn(n,γ)

TABLE I. (continued)

Gamma-Ray Energy (keV)	Parent Nuclide	References	Parent Half-Life	Nuclide of Transition	Gamma Rays per Disintegration	Production Method
1063.7 ± 0.2	^{207}Bi	Ro65,Al53,Ya55	30y	^{207}Pb	0.8	^{206}Pb(p,γ)
569.6 ± 0.1		Ro65,Ba56			1	
835 ± 0.3	^{54}Mn	Ro65	314d	^{54}Cr	1	^{54}Fe(n,p)
661.65 ± 0.1	^{137}Cs	Mu52[d],Li53	30y	^{137}Ba	0.8	Fission
511.003 ± 0.005	(e^+e^- annihilation,sharp component)	Co63,Mu65				
477.4 ± 0.2	^{7}Be	Ro65	53d	^{7}Li	0.1	^{7}Li(p,n)
411.795 ± 0.009	^{198}Au	Mu63,Mu65	2.7d	^{198}Hg	1	^{197}Au(n,γ)
392.6[c] ± 0.8	^{113}Sn	NRC-60-2-105	120d	^{113m}In	0.5	^{112}Sn(n,γ)
319.8[c] ± 0.3	^{51}Cr	Ro65	28d	^{51}V	0.1	^{50}Cr(n,γ)
364.50 ± 0.05	^{131}I	Ho53[d]	8.1d	^{131}Xe	0.8	Fission
284.34[b] ± 0.05					0.06	
80.17[b] ± 0.01					0.03	
279.12 ± 0.05	^{203}Hg	Ed58	47d	^{203}Tl	0.8	^{202}Hg(n,γ)
208.1[c] ± 0.3	^{177}Lu	NRC-59-3-103	6.8d	^{177}Hf	0.1	^{176}Lu(n,γ)
113.02[b] ± 0.05					0.01	
191[c] ± 1	^{114m}In	NRC-60-3-97	50d	^{114m}In	0.2	^{113}In(n,γ)
159.2[c] ± 0.3	^{123m}Te	Co51	110d	^{123m}Te	0.8	^{122}Te(n,γ)
121.97[a] ± 0.04	^{57}Co	Be57,Ch58	270d	^{57}Fe	0.9	^{56}Fe(p,γ)
14.37 ± 0.01		Be57			0.1	

TABLE I. (continued)

Gamma-Ray Energy (keV)	Parent Nuclide	References	Parent Half-Life	Nuclide of Transition	Gamma Rays per Disintegration	Production Method
84.262 ± 0.004	^{170}Tm	Ma63	127d	^{170}Yb	0.1	^{169}Tm(n,γ)
59.59 ± 0.03	^{241}Am	St58	458y	^{237}Np	0.1	

a. Distorted somewhat by a nearby line of weaker intensity.

b. Accompanied by a substantial background from higher energy gamma rays.

c. Inadequate precision or no confirmation, but no nearby isolated line is as convenient.

d. Value from this reference was adjusted slightly to correspond to the 1955 (Co55) or 1963 (Co63) adjustments of physical constants or other changes in the best values of the calibrations used.

Table 2. Energies and Relative Abundances of K X-Rays in ^{109}Ag and ^{203}Tl, from Wa59. Similar data are readily available in Sa58. This table illustrates why care must be used in selection of an effective energy for undiffracted K x rays.

		^{109}Ag		^{203}Tl	
Line		Energy (keV)	Abundance	Energy (keV)	Abundance
$K\text{-}L_{III}$		22.16	1000	72.87	1000
$K\text{-}L_{II}$		21.99	506	70.83	551
$K\text{-}M_{III}$		24.94		82.57	
$K\text{-}M_{II}$	β_1'	24.91	253	82.11	352
$K\text{-}M_{IV}$		25.14		83.04	
$K\text{-}N_{III}$	β_2'	25.46	49	84.92	99
$K\text{-}N_{II}$				84.81	

group is 1/6 for the lighter element and almost 1/4 for the heavier, the consequent distortion of the scintillation pulse-height spectrum is more serious for x rays from the heavier elements.

Figure 1 illustrates the distorted line shape observed for K x rays from heavy elements. For illustration the K_α and K_β components have each been lumped to appear as single lines. The limited energy range within each group allows each component to be represented with small error as a monoenergetic x ray at the average energy of the group.* But use of the average energy of the composite x-ray line structure would be quite hazardous for the example of Fig. 1, since the K_α and K_β groups differ by the full resolution. Stated otherwise, the K_β group is displaced about 1.6 unbroadened standard deviations from the average energy of 74.6 keV. Figure 1 suggests that spectrometrists using undiffracted x rays for calibration should report what effective energies were adopted. Here an "effective" energy is one chosen so that the resulting spectrometer calibration is the same as would have been obtained by using a monoenergetic photon source.

The proper choice of an effective energy depends upon the method to be employed for locating peak positions for energy calibration. Regardless of the method used, the possibility of fabricating the approximate shape of the expected pulse-height distribution allows the following general method to be used for determination of x-ray effective energies.

1. Split the known x-ray line spectrum into at least two groups, and plot on an energy scale the expected pulse-height distribution as

*The following properties hold if two normal distributions having standard deviation σ_o are summed, the first having weight ρ and mean $\bar{p}_1$, the second having weight $(1 - \rho)$ and mean $\bar{p}_2$. The summed (not folded!) distribution
(a) has a mean $\bar{p} = \rho\, p_1 + (1 - \rho)\, \bar{p}_2$,
(b) has a variance $\sigma^2 = \sigma_o^2[1 + (\bar{p}_2 - \bar{p})^2(1 - \rho)/(\sigma_o^2\rho)]$
$= \sigma_o^2[1 + (\bar{p}_1 - \bar{p})(\bar{p} - \bar{p}_2)/\sigma_o^2]$,
(c) may be expressed in terms of $y = (p - \bar{p})/\sigma_o$, $\epsilon = (\bar{p}_2 - p)/\sigma_o$, and $\xi = (1 - \rho)/\rho$ as $f(p)\,dp = dy\,[1 + \xi(y^2 - 1)\epsilon^2/2 - \xi y(2 - \rho)(3 - y^2)\epsilon^3/6\ldots]$ $\exp(-y^2/2)/\sqrt{2\pi}$. For $\epsilon<1$, this expansion implies a shift in the apparent peak position P of $\Delta P = -\sigma_o \xi(2 - \rho)\epsilon^3/3$, measured from the average energy $\bar{p}$, if the peak position is estimated at the ordinate where the distribution has width $2\sigma_o$. Approximations (c) is quite adequate for estimating the effects from superimposed pulse height distributions whenever the quoted three terms of the Taylor expansion are sufficient.

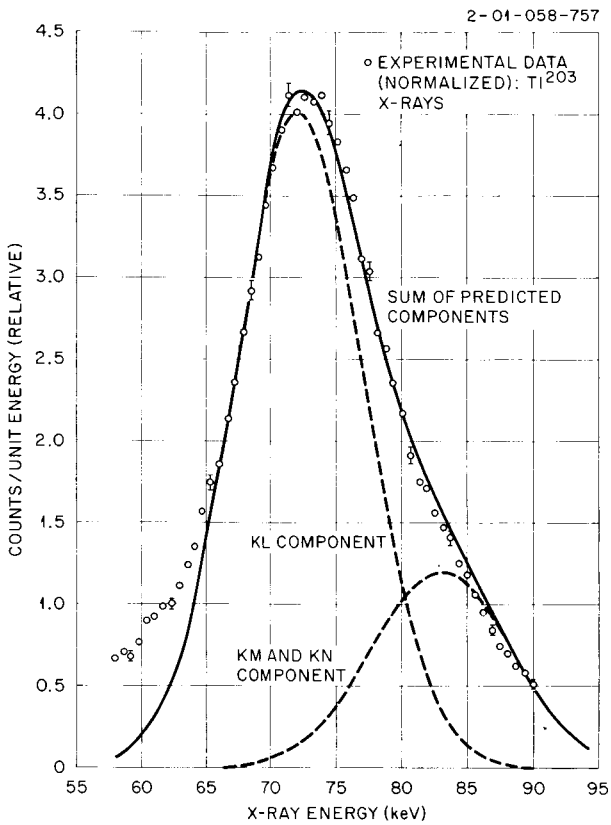

Figure 1. A Differential Pulse-Height Spectrum of ^{203}Tl K X Rays Observed in the Decay of ^{203}Hg. The pulse-height scale is given in energy units. The dashed curves are normal distributions centered at the average energies of the K_α and the K_β x ray groups, with relative areas chosen from the intensity data of Sa58. The (~12 keV) widths of these components correspond to Poisson distributions having three "effective" photoelectrons per keV, "effective" implying that other sources of variance are ignored. The solid curve is the sum of these components. The points are normalized experimental data from a 1-3/4-in.-diam, 1-in.-thick NaI(Tl) detector obtained in coincidence with K-conversion electrons. In the 84-keV region about one third of the discrepancy between points and curve can be explained by the approximation lumping the K-M and K-N x rays, while the tail at low energy is assumed to arise from scattered x rays, photoelectron escape, and iodine x-ray escape. The remaining discrepancy near 84 keV can be explained by uncertainties in the relative intensities of the various x-ray components. (In fact $W_{KMN} = 0.24$ was used in preparing this figure rather than the more favorable value in Table 4.)

the sum of normal distributions, using an instrument resolution appropriate to the spectrometer being calibrated.

2. Apply to the computed spectrum whatever method of peak position location is to be employed on the comparable experimental pulse-height spectra. This yields the effective energy for a particular method, x-ray emitter, and resolution function. While likely weaknesses of the effective energy method are apparent, it does cope realistically with the asymmetric line shape.

Table 3 gives necessary data for x rays from a series of available radioisotopes. Note how the effective energies listed,* chosen for the spectrometer of Fig. 1, differ from the average energy or that of any strong component. So that the reader may conveniently determine effective energies for his own spectrometer, data are listed for a two-component spectral decomposition of each x ray. The given intensity ratios are appropriate when the scintillator detection efficiency is constant over the group of x rays from a given element. For scintillators not too thin, constancy would be assured except for the escape of K fluorescence radiation from iodine atoms in the scintillator. The relative area in the "escape peak" of the pulse distribution depends on the typical depth of penetration of the primary radiation into the scintillator. The effect of escape on the full-energy pulse distribution is therefore largest for lanthanum, barium, and cesium emitters, because for these the iodine K edge (33.17 keV) falls between the K_α and K_β groups of the incident spectrum. Few escapes result for the K_β components, but perhaps 30% of the K_α rays give pulses in escape peaks. Thus the relative escape intensity (see Ax54, Li54, Mo58) for the scintillator geometry employed should be considered in estimating x-ray effective energies.

III. SPECTROMETER INSTABILITY

Spectrometer instability more often limits success in energy calibration than does inadequate data analysis or any other experimental

*For determining these energies, points along the sides of the peaks were fitted to straight lines by eye, and the peak position was taken as the midpoint between these lines at 70% of the maximum ordinate. All components were assumed to have equal efficiency in the scintillator.

Table 3. Calibration of K X Rays from Radionuclides. The emitters below were chosen for their ready availability and usable spectral purity in the energy region involved. E_{KL} and E_{KMN} are the average energies of K_α and K_β x-ray groups, while W_{KL} and W_{KMN} are the combined weights of these groups. E_{avg} is the overall average energy of the K x rays for comparison with E_{eff}, the effective peak energy for the particular spectrometer discussed in the text. Data were derived from Sa58, Wa59, and Nu65. All listed radionuclides may be formed by neutron capture or are separable fission products.

Radioactive Source Nuclide	Emitting Atom	Half-Life	X Rays per Disintegration	PR[a]	E_{eff} (keV)	E_{avg} (keV)	Information for Component Analysis			
							E_{KL} (keV)	W_{KL}	E_{KMN} (keV)	W_{KMN}
^{203}Hg	81^{203}Tl	47d	0.15	7	73.0	74.6	72.15	0.77	82.97	0.23
^{181}Hf	73^{181}Ta	45d	0.2	12	57.9	58.9	57.09	0.79	65.49	0.21
^{147}Nd	61^{147}Pm	115d	0.3	25	39.3	39.6	38.54	0.81	44.00	0.19
^{137}Cs	56^{137}Ba	30y	0.1	9	32.6	32.9	32.06	0.82	36.49	0.18
^{113}Sn	49^{113}In	119d	1	100	24.6	24.7	24.14	0.83	27.35	0.17
^{109}Cd	47^{109}Ag	470d	1.3	200	22.5	22.6	22.10	0.83	25.02	0.17
^{103}Ru	45^{103}Rh	40d	0.1	8	20.5	20.6	20.17	0.84	22.78	0.16

[a]Observed with the scintillator of Fig. 1, the K x-ray spectrum from these isotopes stands above the general background of the neighboring parts of the spectrum by a factor > 6. A typical good-geometry prominence ratio (PR) is given for each nuclide.

difficulty. In the paragraphs below we attempt to bring each origin of drift to the reader's attention and indicate the paths toward its control.

A. Important Origins of Instability

A drift is any unplanned change in the experimental apparatus which alters the mean recorded pulse height for a given energy loss in the phosphor. The destructive drifts are those which occur during an experiment, but continuous drift logging can aid identification of troubles. The pulse-height response of the system is characterized by the system gain, the extrapolated pulse height at zero energy, and any nonlinearity parameters.* The "zero" is usually affected only by electronic drifts in the pulse-height analyzer, but the other characteristics are subject to drifts generated at every link in the chain of energy and signal transfer processes between the gamma-ray interaction and the recorded pulse height.

Fortunately, all possible origins of instability are not important. Nearly all drifts in high-voltage supplies, linear electronics, and pulse-height analyzers can be traced to component decay, input line voltage or frequency changes, temperature or magnetic field shifts, or effects from high counting rates which are generally of an understandable nature. Those drifts in photomultiplier output not produced by dynode voltage or ambient temperature or magnetic field changes are by contrast rather difficult to understand or correct, and tend to provoke demoniacal explanations.

Component decay is less important now than formerly because short-term drifts from scintillator packaging can now be neglected, and transistors do not decay rapidly. However, component drifts in places such as the phototube voltage divider still contribute to the class of drifts never traced to their origins.**

*Some pulse-height analyzers contain a number of drift-sensitive levels, such as edges of individual pulse-height channels. The description given would have to be extended to cover this case.

**Why are carbon resistors still used in phototube voltage dividers?

Power line voltage stability is very important for "vacuumized" electronics because it affects filament temperature. Sensitivity to line voltage is easy to check by varying it with an autotransformer while observing the output. Constant-voltage transformers or other line-voltage-regulating devices can eliminate this source of drift, but the experimenter should familiarize himself with all the specifications of such equipment before using it. Constant-voltage transformers are good for regulation against input changes, typically 1%/15% line change, and may have a temperature regulation of 0.025%/°C. Sometimes, however, they show alarming sensitivity to load shifts, and are rated for as much as 8% change per factor of 2 load change. It is important that variable-load equipment such as timing clocks not be connected onto such regulated supplies. Constant-voltage transformers may change output voltage 2% for a 1% change in line frequency.

Temperature drifts are important both in the linear electronics and in the scintillator-phototube assembly. Typically quoted drifts in both cases suggest the importance of the scintillation spectrometrist becoming an expert in temperature control.

Popular pulse-height analyzers are advertised to have temperature stabilities between 0.3 and 0.2%/°C. Similarly, commercial amplifiers are claimed to have stabilities from 0.01 to 0.1%/°C. Since temperature changes as large as 5°C are hard to avoid in the electronics, the larger coefficients pose a limitation of accuracy.

NaI(Tl) scintillators at the usual activator concentration show marked negative temperature coefficients for both light output and decay time. Startsev et al. (St60) using a particular phototube observed a (-0.12 ± 0.03)%/°C coefficient for crystals of nominal 0.1 mole % thallium concentration for temperatures above 0°C. Startsev also observed a shift in the decay time of the main (0.3 μsec at 20°C) light component of about -2%/°C near room temperature. Thus the observed combined temperature coefficient depends on the operating temperature and the amplifier clipping time. It may also depend on the phototube spectral sensitivity, since Van Sciver (Sc56) has shown a temperature dependence of the NaI(Tl) emission spectrum in the 3500-Å region.

The temperature coefficient of phototubes is confused by the variety of photocathode and dynode materials employed. Furthermore, when tubes are operated at reduced temperature, both the user and the investigator of temperature coefficients may be confounded by the high resistivity of Cs-Sb photocathode material at low temperatures (Rc63). Mott and Sutton (Mo58,p98) summarized the earlier work on popular phototubes, giving values near room temperature from +0.1%/°C to -0.5%/°C. Murray and Manning (Mu60) seem to have resolved the gross discrepancy by studying the response as a function of wavelength, showing that the sensitivity of all the tubes studied shifted toward the blue at low temperatures. Murray's data for tubes with Cs-Sb cathodes appear to show temperature coefficients at 4300 Å [peak of NaI(Tl) emission] in the range -0.12%/°C (RCA-2020) to -0.4%/°C (RCA-6655 and Dumont K-1428) over the temperature region from 0 to 20°C. Since temperature performance may change from one tube to the next of a given type, the differences between the tube types listed may not be real. Murray's results can therefore be interpreted practically (for Cs-Sb photocathodes) as indicating that equipment should be designed for a coefficient of about -0.4%/°C.

Rohde (Ro65a) has recently studied the temperature sensitivity of a NaI(Tl) scintillator and phototube system. He found a variable temperature coefficient of roughly -1%/°C in the region just above 20°C for the tubes studied, with a flatter dependence or even a positive coefficient at slightly lower temperatures. Conner and Hussain (Co60) observed coefficients in the same range. Rohde's results may not be inconsistent with the roughly -0.5%/°C obtained by combining the NaI(Tl) and phototube results quoted in the paragraphs above. In either case detector temperature sensitivity is a primary stability problem.

Magnetic field changes at the phototube can be a serious cause of concern if a fixed energy calibration must be retained while moving the phototube or otherwise altering its magnetic environment.* Most of the sensitivity probably orginates between the photocathode and the first dynode, the magnetic field causing a number of electrons to miss the

*Steel hand tools should not be placed temporarily near a phototube in use.

first dynode. Literature published by phototube and magnetic shield manufacturers never seems adequate for experiment design, so one must perform empirical checks by changing the magnetic surroundings the maximum plausible amount while looking for gain changes. Curves given for some phototubes at one orientation indicate up to a 50% drop in gain when a 1-gauss field is applied, and a few percent shift for a tenth of a gauss (En52, Mi52). Connor and Hussain (Co60) report less sensitivity than this for some Dumont tubes with axial fields, and give some shielding data. Where only the earth's field is concerned, a standard high permeability magnetic shield may suffice.

Count-rate sensitivities are a tricky source of drifts. Under this heading we include effects from changes in averaged pulse current anywhere in the circuit, but not distortions of the spectrum from pile-up effects in which a pulse "rides" close upon the previous one.

First we discuss the effect of high counting rates on electronics.* Ignoring pile-up per se, the most serious effects usually arise from baseline shift (Fa62) in ac-coupled linear stages. This danger has been met by the use of bipolar pulses in many present amplifier designs and by the use of nonlinear baseline restoring circuits in some multichannel analyzer inputs. A baseline shift in the observed spectrum is generated with unipolar pulses if RC coupling leads into a discriminator stage, because the signal voltage across the input resistor will average zero. Thus if 1-μsec unipolar rectangular pulses were employed, a repetition rate of 10^4 pulses/sec would give a baseline shift of 1% of the pulse height. The 1% shift would appear as a zero change to the discriminator, which would still measure from ground potential rather than from the depressed baseline. This analysis assumes that RC is greater than the average pulse spacing.

Numerous designs have been offered for phototube dynode voltage supplies that are claimed to be stable at relatively high phototube

*We neglect the question of overload effects, which has been discussed by Fairstein (Fa62). Here, grid current, transistor saturation, etc., compound the difficulties and can lead to apparent changes in the position as well as the shape of the pulse-height distribution being analyzed.

currents. Nonlinear voltage-regulating elements can be used, but the usual method is to assure that the bleeder current in a conventional resistive divider chain is very much larger than the maximum average phototube current. If phototube currents are not negligible, dynode voltages shift to produce larger phototube gain at high counting rates.* This effect may always be reduced by lowering the high voltage on the electron multiplier and increasing the electronic gain. Voltage on each dynode is normally stabilized during a pulse by means of bypass capacitors, which should be carefully sized to avoid nonlinearity.

Phototube gain shifts and fatigue are induced in the tubes themselves when they are operated at appreciable counting rates. No other difficulty has driven so many workers to the use of automatic stabilizers. In their pioneer 1947 article, Marshall et al. (Ma47) state: "Since fatigue is inherent, its presence must be recognized and dealt with cleverly if the photomultiplier x-ray detector is to be used as a precision instrument.** Fatigue and/or instantaneous shift effects have been shown to depend on photocathode and dynode materials as well as production processes, counting rate, phototube gain, history of usage, and ambient temperature. Though each tube is unique, students have been able to associate typical behavior patterns with given tube types and divide the observed gain changes between nearly instantaneous reversible shift and largely reversible fatigue which occurs over a matter of hours. Each effect can amount to a few percent in experiments at otherwise usable counting rates with tubes from any manufacturer. Migration of cesium, other physical changes in the dynode surfaces, charging of insulators, and more subtle causes have been implicated; and there is

*If the stray photomultiplier anode capacity were 66pF and there were 3×10^4 counts/sec of 1-V charge pulses there, the average phototube anode current would be about 2×10^{-6} A. If a 10^{-4} A bleeder based on 1-megohm resistors were being used with a fixed voltage from photocathode to anode, the average anode current would increase the voltage across the actual dynode structure by about 2 V, enough to cause a >1% increase in the pulse height over that which would have been observed at very low counting rate.

**They recommended low anode currents, 20- to 60-min warmup periods, and alternate measurements against a standard source of about the same intensity. Their advice for dc measurements still applies now for pulse work

evidence that phototube manufacturers are starting to eliminate sources of drift (Rc63, Ko64, Kr65).

The rapid shifts reported by Bell et al. (Be55) seem fully reversible, and by their independence of phototube gain prove themselves to originate in a stage near the photocathode. The logarithm of the shift rises roughly linearly with light intensity on the cathode (Be55, Ju60), and therefore for a given tube the shift depends largely on the average rate of light production in the scintillator. The effect takes its full magnitude within a minute, but there is no literature to indicate whether its relaxation time is 10 sec, 0.1 sec, or 1 msec.* Covell and Euler (Co61a) at about 2.5×10^4 counts/sec of ^{137}Cs report shifts between 0.5 and 10%, with most tested tubes showing less than 1%. Jung et al. (Ju60) report rapid shifts which ranged between ±0.5% for 10^4 counts/sec from the same source, much smaller than the shifts observed on the tubes tested by Bell et al. (Be55).

When the counting rate is increased, fatigue gain drifts appear to have approximately exponential dependence on time with periods up to a few hours. The period depends on the tube, but all workers report that the recovery after the source is removed is slower than the onset for that tube. The recovery period is reported to be lengthened by an extended time at high output current. As noted by Marshall et al. (Ma47) and every author since, the drift seems to occur in the last dynodes of the tube, where currents are highest, and the dc output current is the parameter most correlated to the drift. An equilibrium or quasiequilibrium gain at a given current is reached after a few hours or a day, but after half an hour with 100 nA anode current Covell and Euler (Co61a) report changes between -4% and +10% for various tubes, with a few EMI 9578B and EMI 9536B tubes performing the best. At the same current Jung et al. (Ju60) observed total drifts in the range 0.5 to 2%. These drifts or similar ones were studied by Cathey (Ca58, Ca61) at currents up to 1 μA, but he observed drifts so large that spectrometry would

*Workers with accelerators of low duty factor would presumably have observed alarming shifts and reported them if 1 msec were the relaxation time.

generally be impossible. Cantarell (Ca64) and Cantarell and Almodovar (Ca65) report that for a given tube and temperature the effects are very reproducible and graphically predictable,* and Jung's results quoted above seem to confirm this. When the fatigue cannot be made small by use of low counting rates, the phototube gain should be lowered to reduce the average anode current, though Jung et al. (Ju60) graphically show that the "returns" diminish because at low phototube gain more dynodes play an important role in the fatigue. Cathey (Ca58, Ca61) has shown that ambient temperature and perhaps also the relative electrode voltages near the anode are important in fatigue. Chéry (Ch60) and Karzmark (Ka65) indicate that aging some tubes at dissipation-limit currents (1mA) can improve apparent stability.

Both types of phototube gain change vanish at low counting rate, though turning on the high voltage is said to produce an effect similar to that of using a small source (Ju60, Ca64). The short-term shift remains constant for a given cathode current, and the fatigue after a period of hours reaches a steady value which depends on the anode current. Thus a few-hour waiting period and maintenance of a constant average light intensity are essential in controlling both effects. Fatigue is reduced by lowering the phototube gain, so it appears that for reproducible work without excessive tube testing the average current should be restricted to a few nanoamperes.**

Where high anode currents are required to drive coincidence circuitry, a positive pulse is often derived from a dynode a few stages prior to the anode in hopes of attaining better stability and linearity for pulse-

*Cantarell in fact suggests that an extra-strong source be used to drift a tube rapidly up to carefully predicted equilibrium gain appropriate to the smaller source to be used in an experiment. This would not be much help for a time-dependent source unless an adjustable dc light were used to hold the anode current constant.

**For a typical stray capacity of 50 pF on a phototube anode, and 10^4 counts/sec averaging 5 V at the amplifier output, the average anode current would be 5 nA for an overall amplifier gain of 500. Amplifiers with this maximum gain encourage unnecessary acceptance of fatigue effects unless they are used with a preamplifier.

height spectrometry.* Chéry (Ch60) has observed fatigue at an earlier dynode almost as severe as at the anode, and the resolution (Be55, Co60) under fatigue conditions also suggests that high average anode currents may sometimes be sensed by the whole phototube. In any case, the short-term shifts arising near the cathode would be equally evident at any late dynode.

In summary, experimenters who wish to work with precision as close as 1% can materially simplify their drift problems by following the procedures suggested concerning choice of equipment, care with magnetic field and temperature ambients, and use of constant low phototube currents.

B. Experiment Design to Detect and Avoid Drift

An experiment can be designed to illuminate drifts before much damage is done, to make the results insensitive to drifts, or perhaps even to eliminate drifts.

The most usual method for making drifts unimportant is to measure simultaneously the pulse-height spectra of the energy standards and the unknown source. This is possible when a simple line structure is involved and time dependence is not important. Small drifts in this case cause only a broadening of pulse-height distributions.

Where this method cannot be used, short-term interchange of unknowns with standards sometimes can be used, with perhaps one standard remaining in each of the two pulse-height distributions. This strategy has the strong advantage that a standard energy can be chosen arbitrarily close to an unknown. The interchange method is further discussed near the end of the next section.

In many experiments no particular tricks are possible, so drift must be minimized by separating its sources and attacking them one by one. Drift tracing is aided by recording the phototube supply voltage and the electronic gain, either continuously or periodically.

*In these cases pulse pickup from larger signals near the anode causes difficulty which must be met by critical arrangement and sizing of bypass condensers.

For monitoring high voltage the authors have used a 10-mV strip-chart potentiometer recorder to plot the difference between a standard cell potential and the 1-V position on a precision bleeder from the phototube supply voltage. While this makes simple the required 10^{-4} sensitivity, temperature drifts in the test apparatus may mask power supply changes. This pitfall can be softened by housing the test device in an insulated box to inhibit heat transfer, but a temperature-compensated reference voltage should be employed. Manually operated potentiometers would be adequate except that in practice one forgets to consult with them.

For drift checks, standardized test pulses of shapes similar to those from the scintillator-phototube combination need to be introduced into the electronic system as close as possible to the phototube. Figure 2 shows a pulser connection which the authors have found useful though imperfect.* Pulses thus introduced test the entire electronic system, but for drift tracing one must have standard pulses available for introduction also at the amplifier and pulse-height analyzer input terminals. The ultimate drift tests performed with radioactive sources at useful rates may be commenced when pulser tests show that the equipment is satisfactory. A stable and convenient light pulser would have an important application for this type of work as well as for automatic stabilization.

C. Gain Stabilization

Since the early work of Wilkinson (Wi50), von Dardel (Da55), and de Waard (Wa55), an increasing number of instrument systems are being designed to provide automatic gain and/or zero stabilization. Such systems require that an error signal be generated to indicate the difference between system gain (channels/MeV) and some preset value

*E. Fairstein has noted that the arrangement of Fig. 2 does not allow minimum noise at the preamplifier input because it defeats the usual strategy of using a large R_1. Where grid resistor thermal noise is significant this pulser input should not be used. In scintillation spectroscopy such conditions seldom occur.

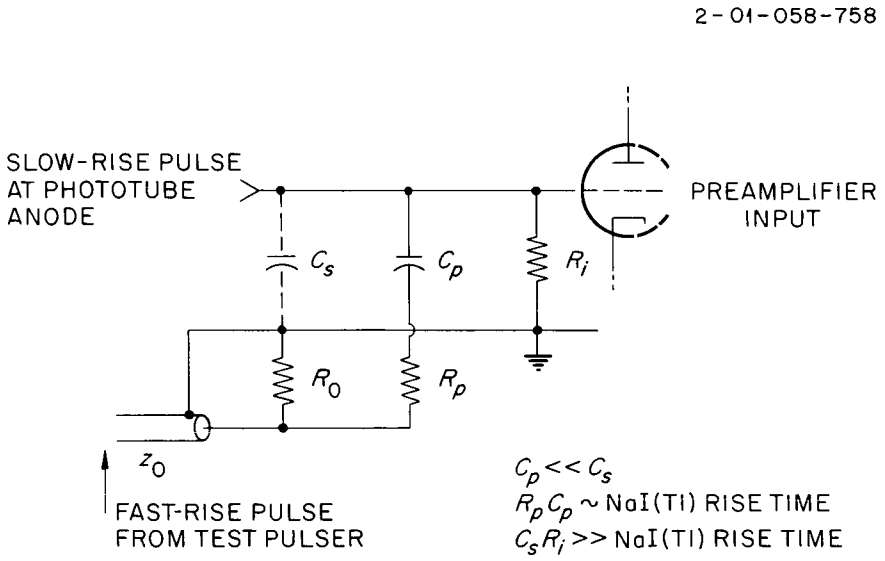

Figure 2. Mixer Circuit for Test Pulses and Phototube (Charge) Output Pulses. By Trimming $R_P C_P$, a pulser signal can be made to resemble that from a NaI(Tl) scintillation counter. The pulse from the phototube may have objectionable overshoot if C_P is not sufficiently small compared with the stray capacity C_S. R_O is chosen to terminate the cable from the test pulser. As drawn, the circuit suggests that the phototube is powered by a negative high-voltage supply. R_i and C_S include all impedances to ground from the preamplifier input.

and that the signal be employed to alter the gain toward a smaller error. Stabilizer systems can be characterized according to how the system gain is estimated, how the error signal is generated, and how the gain is altered.

Valckx (Va61) was able to use the static DC phototube current to indicate phototube gain in pulsed accelerator experiments, and Rijks (Ri61) used a low-frequency-modulated light source, but most workers have employed some sort of light pulse seen by the phototube to include most of the spectrometer system within the gain measurement. A prominent peak in the unknown spectrum may be utilized (see St64 and Di63 for simple systems of this type) if there is no time dependence of any sloped background "beneath" it, but the most flexible systems allow the gain-measuring pulses to be tagged by their pulse shape (Hi64), their coincident radiations (Du64), or the trigger for an artificial light pulse (Ha60, Ke63, Mc65). In a sense only the method of Dudley (Du64) includes the entire system within the gain measurement because others exclude the scintillator. Similarly, as Ladd (La61) and others have noted, the output test-pulse height should be measured through the same pulse analyzer that is used for the spectrum being studied, though the test signals should not be recorded.

The error signal is usually generated from the output pulses that occur in two adjacent pulse-height windows which just straddle the test peak in the pulse-height distribution being stabilized. [One window can be used if the count rate and window width are stable (St64).] The difference or ratio of these count rates can be sensed with an analog rate meter, or an "up-down" counter can record the cummulative difference between the numbers of counts within the two windows and from this produce the error signal with a digital-to-analog converter. Stabilized system performance with an imposed drift, including statistical counting problems, has been considered by Wilkinson (Wi50), by de Waard (Wa55), and Dudley and Scarpatetti (Du64) for analog systems and by Ladd and Kennedy (La61) for a digital system.

The error signal may be utilized by adding it to the high voltage on the photomultiplier if the phototube transit time need not be held

constant for timing purposes. Amplitude-to-time differential pulse analyzers often permit small changes in conversion gain by application of the error signal to the constant current supply which generates the time-measuring ramp. Variable gain amplifier stages have also been employed (Ma62a, St64, Na65).

Zero correction may be combined with gain stabilization if a second smaller pulse signal is injected (Du64) or if the pulse analyzer is triggered to sample the baseline when there is no signal (Ch62).

The stabilization devices, some of which are available commercially, have achieved enough sophistication and ease of use to be practical when large intrinsic drifts are expensive. More work seems required to simplify the generation of tagged pulses in or near the scintillator.

IV. SPECTROMETER LINEARITY

A. Definition and Specification of Nonlinearity

We continue to assume that for every gamma ray of energy E we can obtain the mean voltage or channel number P of the full-energy peak in the corresponding pulse-height distribution N(p). In Sect. V are discussed the methods for finding P. A given spectrometer has linear pulse-height response over the stated energy range if there exist constants a and b such that $P(E) = aE + b$, within experimental error, for gamma-ray energies in some region $E_L \leq E < E_U$. The response is proportional if $b = 0$, though the value of b is rather arbitrary since the pulse height registered for a pulse of zero amplitude is adjustable in most pulse-height analysis equipment. For this reason linearity of an entire spectrometer is usually discussed, though reference to proportionality is more appropriate for the scintillator itself.

Even under the best circumstances, NaI(Tl) gamma-ray scintillators do not yield light-output response proportional within normal experimental error to the energy absorbed. This unavoidable nonproportionality complicates data analysis and limits precision. Nonlinearities in electronic instruments may aggravate this unpleasant situation and also provide a source of drift. To analyze the linearity problem, we will

examine in Sect.IV.B. the proportionality of each of the elements of the chain process which links incident gamma rays with output pulse-height distributions.

For an example of linearity definition, consider the combined electronic gear which connects the magnitude of the charge q liberated at the anode of a photomultiplier to the mean pulse height P observed on a multichannel differential pulse-height analyzer. We assume here that q does not vary statistically, and if noise is small we can ignore the width of the statistical distribution of output p for a given q. To eliminate channel width ambiguity, we further suppose that observations are made for pulse heights which average on the boundary between adjacent pulse-height channels. So we may obtain a series of experimental points (P_i, q_i), and wish to fit them within error to an expression of the form

$$P(q) = aq + b + R(q) \quad ,$$

where a and b are to be chosen to minimize the maximum absolute value of R(q) observed in the range of interest. The integral nonlinearity (Intnon) of the tested equipment is usually defined relative to the full range of possible pulse heights as Intnon = $\pm |R|_{max}/P_{full\ scale}$. Intnon reflects the degree of difficulty the experimenter has in drawing a straight-line calibration relating collected charge q to mean pulse height P.

A complementary quantity is the differential nonlinearity (Difnon). Let d be a constant chosen to minimize the maximum observed absolute value of S(q) in the relation $dP(q)/dq = d + S(q)$. Then usually Difnon = $|S|_{max}/d$. Difnon represents the difficulty encountered by the experimenter in determining from a continuous pulse-height spectrum the true number of pulses per unit range of q.

The quantities Difnon and Intnon are related, since if either is zero the other must be. This relationship depends upon the rapidity of the sign fluctuations in S(q). An analyzer with a ± 33% differential nonlinearity has small integral nonlinearity if alternate channels have twice the width of the intervening ones. On the other hand, Difnon for

a ± 0.5% Intnon is at least four times as large, or ± 2%. This occurs if the lower half of the channels are 2% larger than average and the second half 2% lower than average. So if one observes an integral nonlinearity of ± 0.5% of full scale there is practical assurance that the corresponding differential nonlinearity is greater than ± 2%. The discussion of differential nonlinearity has been included because of its great importance, though the concept of integral linearity is more naturally employed in energy calibration problems.

B. Origins of Nonproportionality

At every step of the energy transfer process between the gamma-ray source and the pulse analyzer there are opportunities for nonproportionality. Some of these may be controlled. The more prominent opportunities are described below, working from the equipment output toward its input. Assume that a single-crystal NaI(Tl) scintillation spectrometer is to be used, though many of the effects occur in more complex spectrometers.

1. Pulse-height analyzers are a significant source of nonlinearity. The currently most popular multichannel types employ input linear amplifiers and gates, followed by a conversion from pulse-voltage amplitude to a time interval measured by using a gated oscillator and a scaler to give the channel number. Manufacturers generally claim integral nonlinearities of no worse than ± 0.5% and differential nonlinearities of no worse than ± 2%, if the lowest few percent of the pulse-height range is ignored. Experience shows that the typical untested multichannel pulse-height analyzer found in the nuclear laboratory must be assumed to be no more linear than the specifications quoted for it at the time of purchase.

2. Linear amplifiers and preamplifiers in common use seldom have important nonproportionality when properly employed. Most deviations are observed near the highest pulses meant to be produced; vacuum-tube systems especially require occasional maintenance to minimize this effect. One should note whether gross pulse-shape changes occur near these highest amplitudes, since pulse analysis equipment is often sensitive to pulse shape as well as maximum amplitude.

3. Multiplier phototube proportionality depends at least on pulses of all important amplitudes sensing the same electric potential distribution throughout the multiplier. This in turn depends on the absence of important space charge effects and upon the supply of stable voltages to all the dynodes. The dynode supply system must be "stiff" enough to furnish the average current drain without appreciable voltage change (< 0.05 V anywhere along the divider), but equivalent stability during a pulse is usually obtained by the use of a series of bypass condensers linking the last photomultiplier stages to electrical ground. Space charge effects can occur during large pulses, though this danger is slight when using NaI(Tl) if phototube gains have been kept small to reduce drift, unless voltage differences between electrodes near the anode are subnormal.

4. Bias in light and photoelectron collections result from differences in the average efficiency of light collection from various parts of the scintillator to the photocathode, and from the illumination of the cathode seldom being so uniform that variations in photoelectron collection efficiency are completely averaged. These nonuniformities are generally discussed in the context of the transfer variance (Br55, Bi58, Ma62). The nonuniformity of efficiency for production of multiplied photoelectrons resulting from these combined effects is important because the considerable absorption of lower energy gamma rays in the scintillator produces a spatial distribution of light production which changes as a function of gamma-ray energy. A nonproportionality is introduced which has not been isolated from others but which may be assumed to be present whenever scanning a mounted crystal with a low-energy source indicates a variation of the mean pulse height with source position. The latter effect has often been observed on large crystals and on those whose length is greater than their diameter.

5. Scintillator nonproportionality has been demonstrated for NaI(Tl) by a number of experimenters: the mean light output from the interaction of gamma rays with a NaI(Tl) crystal is not proportional to the energy lost in the scintillator (En56, Pe60, Ka61, Ka62, Ir62, He65). Zerby, Meyer, and Murray (Ze61) and Iredale (Ir62) have

identified the experimental results with an underlying energy variation of the light production efficiency of electrons, compounded with the manyfold electron-photon cascade in the scintillator. This view is consistent with the existing electron data (Sh64) and with the understanding of the scintillation efficiency vs specific energy loss yielded by Murray and Meyer (Mu61). Commonly in studies of scintillator proportionality one plots the specific light production per unit energy against energy,* though from such a plot numerical values of integral and differential nonlinearities cannot be directly obtained. The data of Kaiser (Ka62) imply integral nonlinearities of $> 1\%$ over the range 15-300 keV, $< 0.2\%$ over the range 0.08-1.3 MeV,** and about 0.5% in the range 10-80 keV.

Scintillator nonlinearity is the most important of the difficulties thus far discussed. Since analysis must be based on the underlying response of the scintillator to electrons, the dependence upon crystal size has not been expressed simply. Furthermore, special spectrometer types such as pair spectrometers do not involve the same series of secondary electron interactions in the crystal as does a single-crystal spectrometer at the same energy, so proportionality of such spectrometers might be observably different.

6. Compton scattering and bremsstrahlung or electron escape involve the nonunique relation between the source gamma-ray energy and the energy loss distribution in a crystal. Compton scattering at a small angle in a thick source or from a collimator between the source and detector can cause the average energy of the photons entering the crystal to be lower than the unscattered photon energy. The fractional effect on the apparent peak position changes with photon energy, so a nonproportionality occurs. The magnitude of this effect is not known to have

*Unfortunately some of the authors cited suggest nonconstancy of L/E as evidence against scintillator "linearity," while according to our more standard definition it demonstrates nonproportionality. Any straight line on a plot of L vs E produces nonconstant L/E unless the line passes through the origin.

**Over this range the NaI(Tl) nonproportionality also appears as a false intercept, zero pulse height seeminly corresponding to about -20 keV. This is a common practical observation (see also En56).

been discussed in the literature, but can be estimated. Suppose that a monoenergetic source of 1-MeV gamma rays is surrounded by a Compton-scattering sheath just 1 mean free path thick, so that 63% of the original gamma rays scatter. In this single-scattering approximation one can estimate that a spectrometer with 5% resolution at this energy would have its apparent peak position shifted by about 1.5 keV if no correction were made for the continuum, depending somewhat on the method used to obtain the peak position.

Similarly, bremsstrahlung or electrons escaping from a scintillator can shift the apparent full-energy peak to a value slightly below that anticipated. The bremsstrahlung effect can be roughly estimated to be about 1 keV for 3-MeV gamma rays on a 2-cm-diam crystal with 4% resolution, but the effect would be larger for smaller crystals or higher energies.* Electron escape is more difficult to estimate.

These effects do not destroy the efficacy of calibrations in the energy neighborhood of the unknown if the geometry is unchanged, but can affect the proportionality of source energy to mean "photopeak" pulse height in a subtle manner.

C. Linearity Test Methods

1. Pulser Tests. -- Integral linearity may be checked using radioactive sources, but precise results are sufficiently difficult by this method that electronic equipment should first be tested using a precision test pulser. The confusion caused by scintillator nonproportionalities can be avoided in this manner until the electronic equipment has been proved usable. The following precautions must be taken in the use of precision test pulsers**(see also Crouch and Heath, Cr63):

*Estimated from Zerby and Moran's (Ze59) bremsstrahlung calculations for 3-MeV electrons, together with escape probabilities from Case, de Hoffmann, and Placzek (Ca53).

**Mercury-switch pulsers are popular for this service. The design must include a time-constant for charging the switched capacitor such that the desired potential actually appears at the capacitor terminals when the switch is activated.

a. Pulses should enter the system between the phototube base and the first circuit element capable of nonproportional behavior, preferably without the detector being disconnected during test measurements. The test pulse should have rise and decay times which match the pulses from the phototube.

b. A sufficiently high-quality attenuator or voltage control (or readout) must be employed.

c. If the pulser has active elements between its output and the point of precision pulse generation, these circuit elements must be proportional beyond question. Such intermediate circuits are sometimes employed to provide flexibility of output pulse shape.

d. The custom of using line-frequency repetition rates should be discouraged, since line-frequency pickup can displace the pulse height "zero" of pulse-height analysis systems. Introduction of a spread in pulse heights from this noise would be preferable.

e. If the distribution of pulse amplitudes is narrower than one channel, some plan must be followed to allow determination of the fractional-channel value corresponding to the average pulse height. Some workers introduce noise on the signal to produce a distribution wide enough to be easily plotted, but the authors prefer to observe a dynamic channel-address indicator while adjusting the pulse amplitude until the storage rate is shared about equally between adjacent channels. In this manner no error larger than 0.2 channel will likely be made. Crouch and Heath (Cr63) describe a more precise extension of this approach.

f. At least 15 points should be taken for a careful check, perhaps with a concentration at low pulse heights where nonlinearities often appear. The pulse amplitudes should not be chosen in a monotonic sequence.

Differential linearity is of most interest when spectral intensities (counts per MeV or per volt) must be determined in a continuous spectrum, but a good test of differential linearity may be integrated to produce a

precise test of integral linearity (electronics only*).

Differential linearity tests may be performed by differencing very precise integral data or by using a pulser which yields pulses shaped properly and distributed uniformly over the pulse-height range employed. At a low (60, perhaps up to 250, counts/sec) repetition rate this may be done by applying a linear voltage ramp from a low impedance source to a mercury switch pulser. A special circuit may be constructed (Wo65) or a slow (50- to 100-sec) sweep from a standard laboratory oscilloscope may be used. The linearity of the voltage ramp may be tested using a differentiating circuit designed to produce a small (~10-mV) voltage output appropriate to drive a potentiometer-type chart recorder. Except for the very first part of the sweep before the response time of the recorder is exhausted, the recorder should indicate a constant voltage during each sweep. With such a system many hours are required to obtain an adequate number of counts. Unfortunately, most pulsers having higher repetition rates do not have the simple properties of the mercury switch; alternate designs require considerable pains be taken to assure the equal distribution of output pulses.

An alternative approach produces a flat spectrum of pulses by the use of a perfect time-to-pulse-height converter coupled with a random time-interval generator such as a radioactive source (Dr59). This is a splendid concept, but it is hard to obtain a time-to-amplitude converter with independently testable or completely reliable linearity.

2. Integral Linearity Tested with Gamma-Rays of Known Energy. -- When the electronic equipment is working well enough, the energy calibration of the system may be studied using gamma rays. Precautions must

*It is often suggested that the rather flat spectrum of pulse amplitudes observed in the Compton tail region with a source such as ^{60}Co might be used to study differential linearity. Since the expected spectrum shape is imperfectly known, the pulse spectrum must be studied at different electronic gains. This method would be quite valuable if it covered the whole range of pulse heights needed to be tested and if there were no ambiguity in the "zero" of the pulse analysis system. Such a test is excellent for detecting an "odd-even" nonlinearity in which alternate channels are wider than the intervening ones.

be taken to avoid drift and nonlinearity, so such an exercise is uneconomical except for the calibration of the energy scale for some experiment. Here we review the steps to be taken to minimize effects of drift and expose the needed information concerning the energy scale.*

a. Pulse-height spectra from a series of gamma rays of known energy must be studied, with one calibration point as close as possible to the energy of any discrete unknown peak. If a broad spectrum is to be studied, calibration sources must be scattered over its entire energy range.

b. Popularly the pulse spectra from unknowns and energy standards are measured simultaneously to avoid drift effects, as described in Sect. 3. They must also be obtained separately or with one source at a time removed so that proper subtraction of the residual spectrum "underneath" a given peak may be performed. This method frequently prevents use of the nearest possible calibration, and cannot be used for continuous spectra.

When the spectrum being studied is complex or widely distributed, the source-interchange method is required. The intensities of the two sets of gamma sources should be arranged so as to keep the average phototube anode current constant** and rather low (1×10^{-9} amp). Source sets must be interchanged more than once to expose drift, and results are most conclusive if one gamma ray can be retained as a member of each set.

c. Calibration sources should be placed in geometry similar to that of the unknown source so that any geometry-sensitive nonproportionalities will occur in the calibration.

The above precautions may be relaxed whenever maximum precision is not required.

*The corresponding data analysis problem is taken up in sect. V.B.

**Note that on pulse-height analyzers which convert pulse amplitudes to time intervals the ratio of "live time" to clock time is a convenient measure of the average anode current, if the effect of the fixed storage time is compensated for.

D. Data Reduction to Compensate for Nonlinearities

The above discussion shows that nonlinearities should be observed in a careful gamma-ray experiment unless the energy range is small or the sources of nonlinearity somehow compensate each other. To avoid serious ill effects in the results, one of three overlapping approaches may be used:

1. The energy vs pulse-height calibration may be restricted to so small an energy range that local or tangential linearity may be assumed. This simple method is highly esteemed where it is applicable (see Pe60a).

2. The calibration data may be fit with some appropriate or guessed functional form. Calibration data typically can be more nearly fit to a P vs E relation which includes one or more nonlinear terms (Ju62, He65). The form of the nonlinear term is usually arbitrary, leading to some conceptual difficulty because the statistical analysis of fitting procedures assumes that the chosen functional form is capable of precisely fitting the expectation values of P_i.

3. A priori information can be used to remove nonlinearities from the data prior to establishment of an energy scale.* One hopes here that that the uncompensated nonlinearities may become insignificant, or at least that method 1 above may be applied over an enlarged energy range or that the amplitudes of nonlinear terms 2 may be diminished.

Methods 1 and 2 are discussed in Sect. V.B. Here we discuss method 3, preferred by us when method 1 is inadequate. Analysis of the electronic nonlinearities is stressed, but information from the references on scintillator nonproportionality should be superposed.

The purpose of this approach is to obtain for each pulse height p a transformed pulse height $p'(p) = p + \Delta(p)$ such that on the new p'

*Equivalently, the nonlinear term can be specified in detail on the basis of a priori information.

scale photopeak positions can be expressed as a linear function of gamma-ray energy over the desired range of E. In practice one needs the equivalent of a plot of $\Delta(p)$ vs p to perform this transformation on both unknown and calibration spectra. Such a linearization technique is practical in the case of electronic nonlinearities, provided these nonlinearities are sufficiently stable to allow the use of pulser calibration data.* If very good integral pulser data are available, one can draw (implicitly or actually) an arbitrary straight line among the points, plot the deviations from this straight line as a function of pulse height, and interpolate between them to evaluate $\Delta(p)$.

If good differential linearity data are available, a more precise correction can be made. Let n_k be the observed count in channel k, $\bar{n}$ being the average over the whole spectrum. We assume for convenience that the analyzer counts properly even in the lowest channels.** The purpose is to transform the pulse-height coordinate to $p'(p)$ in such a way that in the new system a unit channel would collect $\bar{n}$ counts. Then a linear relationship $p' = av + b$ will hold in the transformed system, where v is the pulse amplitude at the input to the electronic system. Differential linearity data yield information on the transformation for half-integral values of pulse height $p = k + 1/2$, using the definition that the integral channel number is assigned as the value of the pulse height in the center of each channel:

$$p'(k + 1/2) = 1/2 + \sum_{m=1}^{k} n_m/\bar{n} \quad . \tag{1}$$

Values for $p \neq k + 1/2$ must be interpolated. The variance or mean-square error in p' can be derived for the case of a random-amplitude pulser:

$$V\,[p'(k + 1/2)] = S_k\,(N - S_k)/[(\bar{n})^2\,N] \quad , \tag{2}$$

*The authors have experienced most of their difficulty in matching well enough the shapes of the test and NaI(Tl) pulses.

**Attention may be concentrated on any desired range of channels by a slight extension of the method given.

where N is the total number of counts stored in the analyzer and

$$S_k = \sum_{m=1}^{k} n_m \quad .$$

With reasonable sliding pulser data Eq. (2) gives a great overestimate of the variance because statistical errors arise only in the sorting of counts between channels. Thus the uncertainty in $p'(k + 1/2)$ is something like $\sigma(n_k)/\bar{n}$, where $\sigma(n_k) \leq \sqrt{n_k}$, depending on the amount of noise.

With either of the methods of linearization described above, it is important to keep track of the spectral intensities when the unknown spectrum is continuous. To determine the number of counts per MeV, a smooth approximation must be made to the $\Delta(p)$ vs p curve. Purely statistical fluctuations must not be allowed unless they are relatively smaller than those in the spectrum of the "unknown."

E. The Importance of Linearity Corrections

The magnitude of errors if nonlinearities are ignored can be estimated by assuming that the pulse-height analyzer and NaI(Tl) nonlinearities are dominant. If one straight line is chosen to represent P_i vs E_i for the whole energy range from 0.05 to 2 MeV, errors up to 10 keV must be expected. So large a systematic error would be most serious if limiting precision near 0.2% of an unknown energy were desired. However, if the calibration is confined to a quarter of the pulse-height range, a local linear approximation is apt to approach the required integral precision.

V. ENERGY ANALYSIS OF PULSE-HEIGHT SPECTRA

We suppose that pulse-height distributions $N_i(p)$ are available from each of a series of gamma-ray emitters of energy E_i, and we wish to derive from these distributions an unknown energy E for which a pulse-height distribution is also available. Energy calibration for a continuous unknown spectrum is an extension of this problem. Only the full-energy peaks are to be considered in the analysis, though information can sometimes be derived from other features of the distributions.

The subsections below indicate the steps required to obtain a single pulse height P_i to represent the pulse-height distribution from each gamma-ray energy and to interpret the resulting data couplets (P_i, E_i) to yield the gamma-ray energy and uncertainty corresponding to a full-energy peak centered at any pulse height P.

A. Choice of the Pulse Height P_i to Represent $N_i(p)$

1. Isolation of the Pulse-Height Spectra from Individual Gamma Rays. -- The distribution from the gamma ray of energy E_i will generally be accompanied by some laboratory background and by interfering counts from other gamma sources simultaneously exposed to the scintillator. Such backgrounds should be subtracted prior to analysis for calibration. While pulse-height analyzers frequently allow background to be subtracted without use of an external data storage medium, such internal subtraction should be avoided unless one of the parent distributions is also recorded to allow analysis of statistical uncertainties.

When a single nuclide emits more than one gamma ray, isolating all the pulse-height distributions generated by individual source energies is difficult unless coincidence methods can be used. The effects of one gamma ray on the peak distributions of the others must in this case be removed, using interpolated information on the spectrometer response. Fortunately, only the region within two or three standard deviations of each full-energy peak is needed for analysis.*

2. Determination of the Peak Position P_i from the Corrected $N_i(p)$. -- We now consider an isolated pulse-height distribution for a gamma ray of energy E_i. Given this discrete distribution $N_i(p)$, which frequently approximates values taken from a normal distribution G(p), we wish to choose P_i. One can estimate the average pulse height, the mode of the distribution, or some other convenient measure. In any case, the purpose is to choose a reproducible scheme for a given experiment which can be used with all the full-energy distributions to be

*Some of the peak analysis methods described in this section will yield a result even if this peak isolation procedure is not followed, because a constant background has been implicitly assumed.

intercompared. There is no need to determine P_i more precisely than the experiment warrants, so drifts and other calibration difficulties should be roughly evaluated before any complicated method for finding the P_i's is initiated.

When only the peak position is desired, the effects of finite pulse-height channel width can nearly always be ignored.*

Throughout, a pulse height is indexed at its center, i.e., pulse height p is in channel k if $k - 0.5 < p < k + 0.5$.**

a. Graphical methods. -- The optimum choice among the possible graphical methods may depend on whether other parameters of the full-energy peak are needed. Each of the three methods below yields information on the breadth of the pulse-height distribution, but this potential output is not discussed. Any one of the methods could also provide the basis for a digital computer program which could include an objective error estimate.

The simplest method is to plot the data and some of the statistical errors on linear paper as in Fig. 3a, using at least 1/8 in. per channel. The points along the sides of the peak seem to fall on straight lines, since, if the frequency function is normal, there are points of inflection at $P \pm \sigma$. Let the frequency function of counts per pulse-height interval be denoted by

$$G(p) = \left\{\exp\left[-(p - P)^2/2\sigma^2\right]\right\}/\sigma\sqrt{2\pi} \quad . \tag{3}$$

If we expand G(p) around $p = P + \sigma$ using the variable $(p - P - \sigma)/\sigma = x$, one obtains for small x

$$G(x) \cong G(P + \sigma)\,[1 - x\,(1 - x^2/3) + \ldots] \quad , \tag{4}$$

*If a normal distribution of unit standard deviation is integrated over channels of width δ centered at an abscissa p from the mean, the observed count may be approximated by the following expansion:

$$C(p) = (\delta/\sqrt{2\pi})\exp(-p^2/2)\,[1 + (\delta^2/24)(p^2 - 1) + (\delta^4/1920)(3 - 6p^2 + p^4) + \ldots] \quad .$$

**Other definitions are common; so, reader, be wary.

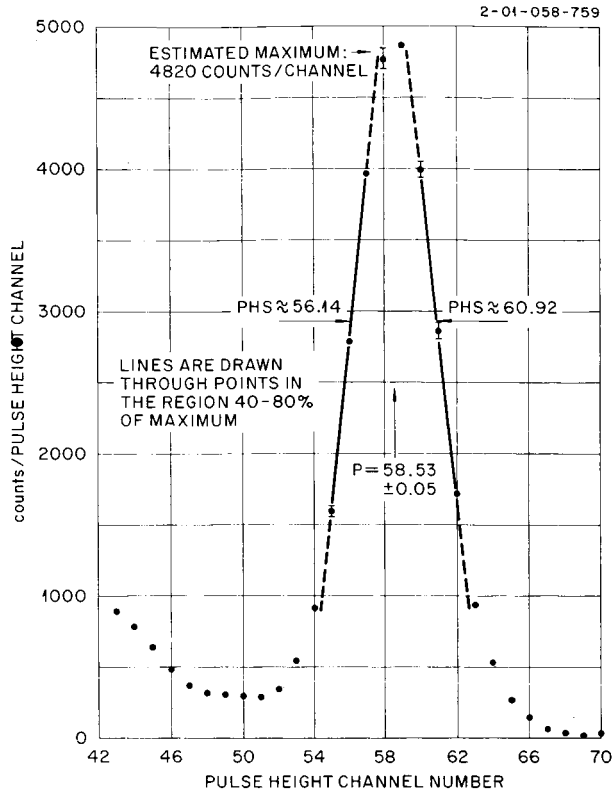

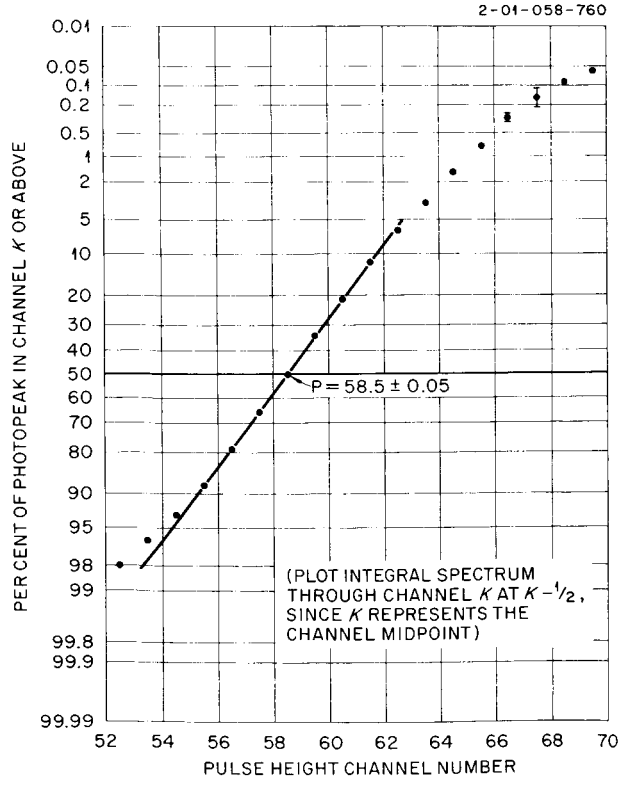

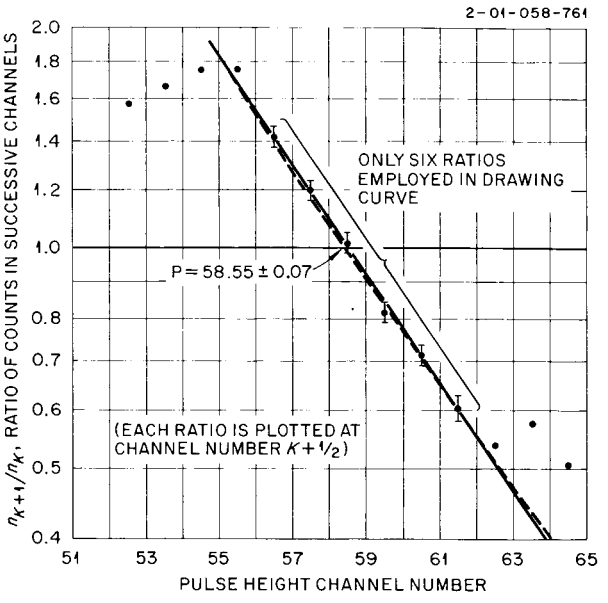

Figure 3. An Illustration of Graphical Methods for Determining a Photo-Peak Position, Using an Experimental Spectrogram of the 0.9-MeV Gamma Ray in the Decay of ^{88}Y. (a) A plot of the differential spectrum, with straight lines fitted to the sides of the peak in the neighborhood of the inflection point. The value of P is estimated to fall midway between the fitted lines at 61% of the maximum intensity. (b) A plot of the normalized integral spectrum on linear probability paper. P is estimated as the intercept of the line fitted to the data points with the 50% ordinate, corresponding to an apparent bisection of area. (c) A semilogrithmic plot of ratios of observed intensities in successive channels, from which P is chosen as the intercept with unit ratio. The dashed line has the shape predicted for a Poisson distribution having the same relative resolution as the data.

The errors shown on all estimates of P are qualitative, based on the uncertainties experienced in drawing the curves. Only for case c was a small approximate background subtracted (18 counts/chammel).

where the next term contains x^4. Thus the idea of straight-line relationships along the sides of the peaks is justified within ~8% in the region $|x| < 1/2$, where G(p) is between 33 and 88% of its maximum value. If this method is used, it is most reasonable to take as the estimator of P the midpoint between the straight lines at the ordinate given by $G(p)/G(P) \cong 0.61$. At this ordinate the distance between the lines is about 2σ. If there are at least two data points in the regions where the straightline approximations are valid and if the slopes of the lines on either side are nearly equal in magnitude, the method is a very good one for hand calculation. The result for P is not influenced by a constant background, and even when the observed pulse-height distributions are asymmetric, this method seems quite reproducible.

A second graphical method (Bo60, Zi61) employs linear probability paper, on which the error integral $I(e) = \int_e^\infty G(p)\, dp$ appears as a straight line when plotted against e, where G(p) is the normal distribution of Eq. (3). The method assumes that the background-free data are sampled from a normal distribution and that the area of the experimental peak can be determined for normalization. To plot the example shown in Fig. 3b, the area of the experimental distribution was estimated by summing the counts in the peak, though such a sum always involves guesswork in the valley between the full-energy peak and the Compton edge. The partial sum down through the kth channel, to be plotted at $p = k - 1/2$, is just

$$I(k - 1/2) = \frac{1}{A} \sum_{k}^{K} n_k \quad , \tag{5}$$

where K is chosen as an arbitrary upper cutoff for counts presumed to be associated with the gamma-ray peak in question, and A is the estimated area of the whole distribution. P is taken as the fractional channel number at the intercept of the plotted line with $I = 1/2$. This method has the advantage of combining the observed data in all the channels in a simple integral manner, but the advantage is coupled with a difficulty in determining A whenever the valley to the low pulse-height side of N(p) is poorly determined. A relative error $\Delta A/A$ in the estimated area

should produce a peak-position error $\Delta P = 1.25\sigma\Delta A/A$, so a 2% error in area typically can be tolerated. In drawing the curve one must remember that the statistical uncertainties in the plotted points are very highly correlated.

The third scheme, proposed by Zimmerman (Zi61), requires a semilog plot of the ratios of the contents of successive channels. If the pulse-height distribution were normal, the line which approximates the plotted ratios should intercept unity for $p = P$. To see this, define $R(p) = \frac{N(p + 0.5)}{N(p - 0.5)}$. Assume first that $N(p) \cong G(p)$ near its mean. Then in the normal approximation

$$R(p) = \frac{G(p + 0.5)}{G(p - 0.5)} = \exp\left\{\frac{-1}{2\sigma^2}\left[(p + 0.5 - P)^2 - (p - 0.5 - P)^2\right]\right\} ,$$

or

$$\ln R(p) = \frac{P - p}{\sigma^2} . \qquad (6)$$

This straight line crosses $R = 1$ when $p = P$. Such a line may be drawn from the known values of the ratio at each channel edge; i.e., the contents n_k of channel k and n_{k+1} of channel $k + 1$ may be combined to estimate ratios at half-integral channels as follows:

$$R(k + 0.5) \cong n_{k+1}/n_k .$$

This formula assumes that the channel contents approximate ordinates of the normal distribution, making the zero-order small channel-width approximation given in the footnote at the beginning of Sect. A.2. An error estimate for the resulting value of P could be made by propagating the counting errors through ln R and then through a least-squares analysis for the best intercept of the line [Eq. (6)]. In estimating errors by simple methods, one should use a given n_k in only a single ratio instead of the possible two in order that the plotted points considered be independent. Otherwise, the strong correlations should be taken into account in drawing or computing the line. The method is illustrated in Fig. 3c. Note that channel contents ratios taken far from the peak

do not fall near the line because the shape of the pulse-height distribution is not nearly normal, and that the value of P estimated for this case will depend markedly on just which channel ratios are employed in drawing the curve. Figure 3c also illustrates that a Poisson pulse-height distribution with about the correct position and breadth would yield count ratios falling on a curved line, so that an estimate of P based on a straight line is generally slightly biased.

b. Use of the mean pulse height. -- The mean pulse height of a peak would be expected to be an efficient method of obtaining P from n_k. This value is given simply by

$$P = \sum_{k=K_l}^{K_u} k n_k \Big/ \sum_{k=K_l}^{K_u} n_k \quad , \tag{7}$$

where the cutoffs K_u and K_l must in practice be chosen to minimize any bias in P caused by unsubtracted backgrounds or the continuum below the full-energy peak. The evident arbitrariness in the selection of these sum limits seems to have reduced the use of this method, but the difficulty is not really so great unless the channels are very wide. One may estimate the maximum bias by observing the effect on the P from Eq. (7) of adding (or substracting) one and two channels from the region included between K_u and K_l. It is assumed that this region will be chosen as symmetrically as possible around the approximate peak position, and the final effect of any bias can be reduced by reaching similar range-of-summation decisions on all the full-energy peaks studied. From the data of Fig. 3 estimates of P based on Eq. (7) are shown in Table 4 using data from the indicated channel intervals. In this approach we have not used an approximate analytic shape for the pulse-height distribution, as required in the development of many methods.

Standard errors for the P of Eq. (7) may be estimated by taking the square root of the variance estimate

$$V(P) = \frac{1}{A^2} \sum_{k=K_l}^{K_u} (P - k)^2 \, n_k \quad , \tag{8}$$

Table 4. A Comparison of Numerical Methods for Estimation of Peak Position, Using the Same Data Illustrated in Fig. 3. The typical stability of the solution as a function of the channels included is demonstrated. Ranges above and below the dotted lines would not normally be tried, on one side containing less than 85% of the data and on the other including regions of obvious asymmetry.

		Nonlinear Fits	
Channel Range	Mean Pulse Height, Eqs. (7) and (8)	3 Parameters, Normal Distribution	1 Parameter, 1 Iteration, σ=2.5 channels, A=3.00 x 10^4
57 - 60		58.52 ± 0.04	58.52 ± 0.04
57 - 61		58.53 ± 0.035	58.49 ± 0.03
56 - 61	58.51 ± (0.010)[a]		58.53 ± 0.03
56 - 62	58.76	58.53 ± 0.022	58.50 ± 0.02
55 - 62	58.53 ± (0.012)[a]	58.54 ± 0.018	58.55 ± 0.019
55 - 63	58.63	58.56 ± 0.017	58.54 ± 0.018
54 - 63	58.53 ± (0.013)[a]	58.54 ± 0.016	58.54 ± 0.016
54 - 64	58.63	58.56 ± 0.016	58.46 ± 0.016
53 - 64	58.53 ± 0.014	58.54 ± 0.016	58.54 ± 0.015
53 - 65	58.59	58.55 ± 0.015	58.55 ± 0.015
52 - 65	58.51 ± 0.014	58.53 ± 0.015	58.53 ± 0.015
52 - 66	58.55	58.54 ± 0.015	58.54 ± 0.015
51 - 66	58.48 ± 0.015		58.53 ± 0.015
51 - 67	58.49	58.52 ± 0.015	58.53 ± 0.015

[a]See text for explanation of these estimates.

where

$$A = \sum_{k=K_1}^{K_u} n_k \quad .$$

Errors thus calculated are listed with some of the values given in Table 4. The largest contributions to the sum of Eq. (8) come from channels 55 and 62 at about one-third of the peak intensity. (For a normal pulse-height distribution it would be at about 37% of the maximum value.) Note that the statistical uncertainty in this estimate of P is small, illustrating both the statistical efficiency of the method and the relatively large importance of the bias uncertainty discussed above. The uncertainty estimates in parenthesis are implausibly small, since using a smaller share of the available data should not reduce the uncertainty. The estimate given by Eq. (8) unrealistically assumes that there are no pulses outside the channel region $K_1 \leq k \leq K_u$.

c. A least-squares curve-fitting method. -- This section describes a technique of nonlinear least-squares fitting (Ch63, Bu62) which normally requires the use of a fast digital computer, though it is slightly adaptable for hand analyzis. Putnam et al. (Pu65) give a similar method, and Julke et al. (Ju62) describe the application to this problem of a slightly different general least-squares scheme similar to that described by Deming (De44).

We wish to approximate n_k in the region of the full-energy peak by a function of pulse height which contains a set of parameters b_σ. One of these parameters will represent the desired peak position P. Let I be the total number of data points to be fit and Σ the total number of parameters required. The basic approximation may be written

$$n_k \cong f(k;\ b_1 \ \ldots\ b_\Sigma) = f(k;\ \underline{b}) \quad , \tag{9}$$

where $\underline{b}$ represents the vector of Σ parameters b_σ. Equation (9)* involves

*Equation (9) can of course be generalized so that the independent variable need not be the channel number.

the scatter of experimental points about the fitted line and the suitability of the function f, which may, for instance, be designed to include the effect of finite channel widths in fitting the data near the full-energy peak. Unless the function f is linear in parameters b_σ, most unusual in this application, iteration must be performed on a second approximation, which linearizes the dependence on the parameters for small differences therein:

$$f(k; \underline{b}) \cong f(k, \underline{b}^0) + \sum_\sigma \beta_\sigma \frac{\partial}{\partial b_\sigma} [f(k, \underline{b}^0)] + \ldots \quad . \tag{10}$$

Equation (10) represents the constant and linear terms in the Taylor series expansion of f in small $\underline{\beta} = \underline{b} - \underline{b}^0$.

The procedure involves a solution for the parameter differences $\underline{\beta}$ by the method of weighted least squares. Reasonable estimates, $\underline{b}^0$, must be available to begin, and iteration is continued by choosing the $\underline{b}^0$ for the (M + 1)th iteration as the $\underline{b} = \underline{b}^0 + \underline{\beta}$ from the Mth iteration. Iteration is usually made to stop when the sum S over all the data points of weighted squared residuals no longer becomes smaller:

$$S = \sum_k w_k [n_k - f(k; \underline{b})]^2 \quad , \tag{11}$$

where

$$w_k = (\text{variance of } n_k)^{-1} \equiv [V(n_k)]^{-1} \quad .$$

If no appreciable background has been subtracted, one normally takes $V(n_k) = n_k$, or sometimes $V(n_k) = f(k, \underline{b}^0)$. The second ought, in principle, to be preferred once the estimates $\underline{b}^0$ are reasonably correct, but in the typical case in which the tails of the function f do not fit the data well, $V(n_k) = n_k$ is more successful.

Derivation of formulas to solve for the β_σ in each iteration proceeds just as for the parameters themselves in linear least-squares theory. We define the matrix $\underline{F}$ with elements

$$F_{k\rho} = \frac{\partial}{\partial b_\rho} [f(k, \underline{b}^o)] \quad , \tag{12}$$

where the notation implies that the derivatives are to be evaluated at $\underline{b} = \underline{b}^o$.

The least-squares matrix $\underline{Q}$ has elements defined as

$$Q_{\sigma\rho} = \sum_k F_{k\rho} F_{k\sigma} w_k \quad , \tag{13}$$

provided only that important statistical correlations have not been introduced among the data counts. Then if $\underline{Q}$ has an inverse, the solution is written in matrix notation as

$$\underline{\beta} = \underline{Q}^{-1} \, \underline{r} \quad , \tag{14}$$

where $\underline{r}$ is the vector with elements

$$r_\sigma = \sum_k W_k F_{k\sigma} [n_k - f(k, \underline{b}^o)] \quad . \tag{15}$$

The summations in Eqs. (13) and (15) are over all the data points included for analysis. Assuming f can fit the data within error one can estimate the variance matrix of the $\underline{b}$ vector based in the usual way on the input weights W_k, as

$$\underline{V}(\underline{b}) = \text{expectation value } (\underline{\delta b} \; \underline{\delta b}^T) = \underline{Q}^{-1} \quad . \tag{16}$$

The outlined procedure is quite convenient once it is programmed because:

1. The form of $f(k; \underline{b})$ is open to a wide range of possibilities. Nonnormal distribution can be utilized, and low-energy tails and even backgrounds can readily be included into the parameterization. (Ch63).

2. One can assure that all the peaks under consideration are fit to the same shape.

3. Other features of the distribution, such as width and area, are estimated along with the peak position P.

4. The goodness of fit of the data to the chosen peak shape can be tested against the chi-square distribution by examining the minimum value of S attained.

5. The output error estimates for the parameters are an objective propagation of the input statistical errors.

6. Interfering pulse-height distributions sometimes can be fit along with the main peak by using a larger number of parameters.

The relative disadvantages of the curve-fitting method include the time that is sometimes required to obtain a suitable machine program, the difficulty in finding an economical parameterization capable of fitting good data in detail, and the likelihood that systematic errors in shape will govern output uncertainties more than the propagated input errors even if drifts are small. If the empirical shapes cannot be fit precisely in the tails of the full-energy peak, the obtained estimate of P will depend on how many experimental points are employed in the analysis.

A machine program employing the method described above was used to approximate the data of Fig. 3 by a normal density function, which requires parameters for the area A, the standard deviation σ, and the peak position P. The results for P are listed in the second column of Table 4.* Note that the estimate of P is fairly stable as different reasonable choices of channels are made and that the uncertainty estimate varies sensibly with the amount of data used. However, the data are not normally distributed, and values of S from Eq. (11) became unduly large (greater than four times the number of degrees of freedom) when more than the ten central data channels were employed. Good fits were obtained with essentially the same value of P when a fourth parameter representing a constant "background" was included.

*For the channel range 54-63, the other parameters were A = (2.95 ± 0.02) x 10^4 counts and σ = (2.43 ± 0.02) channels.

After one of the graphical methods has been employed, a highly simplified least-squares check can be made by hand to obtain a small refinement in P. Suppose again that the normal distribution, Eq. (3), is to be used with an area A estimated by summing the counts in the peak. A reasonably good value of the standard deviation σ is required from the graphical analysis. One takes as P_o the value supplied by a graphical method and performs the least-squares fit in only one parameter, the peak position. In the above notation we have

$$f(k;\, P_o) = A \exp[-(K - P_o)^2/2\,\sigma^2]/\sigma\sqrt{2\pi} \quad ,$$

and

$$r = \sum_k w_k \frac{\partial f(k;\, P_o)}{\partial P}\left[n_k - f(k;\, P_o)\right]$$

$$= \sum_k w_k \left[n_k - f(k;\, P_o)\right] f(k;\, P_o)\,(k - P_o)/\sigma^2 \quad , \qquad (18)$$

where $f(k;\, P_o)$ is the estimated count in channel k if P_o were the peak position. The $\underline{Q}$ matrix becomes a scalar,

$$Q = \sum_k w_k\left[\frac{\partial f(k;\, P_o)}{\partial P}\right]^2 = \frac{1}{\sigma^4}\sum w_k (k - P_o)^2\, f^2(k,\, P_o) \quad , \qquad (19)$$

as does the parameter refinement $P_1 - P_o = r/Q$ from Eq. (14). The standard error in P is just $Q^{-\frac{1}{2}}$. When the subtracted background is not large, one may take $w_k = 1/n_k$.

The third column of Table 4 contains the results for P_1 after one single-parameter iteration as described above. Estimates $\sigma = 2.5$ channels, $P_o = 58.5$ channels, and $A = 3.00 \times 10^4$ counts were used; values of f were computed by hand with the aid of tables of the normal frequency function. Observe that the resulting values and errors are quite close to those from the three-parameter converged iterative fit, possibly because the original estimates were rather close. The estimated standard errors are

the same because in the full procedure the correlations between the computed parameters are very small -- i.e., the 3 x 3 least-squares matrix $\underline{Q}$ has diagonal elements whose inverses are nearly the elements of the inverse matrix. (This is not generally true in fitting more complex functions). It is really not necessary to compute the standard error for each case, since if essentially all the peak is utilized and if the data fit even in the tails, the summation for Q can be readily approximated by an integral to yield $\sqrt{Q^{-1}} = \sqrt{\sigma^2/A} = 1.44 \times 10^{-2}$ channel in the above example.

d. A comparison of methods for finding P. -- Unless the worker must carefully fit the shapes of all his pulse-height distributions, for which a nonlinear fitting code might be useful (see Ch63), the authors recommend the use of the simple linear plot or its automation on any available digital computer. The most important reason beyond simplicity for this choice is that spectrometer responses of imperfect symmetry are handled quite naturally.

It is interesting to compare in Fig. 3 and Table 4 the graphic and numeric estimates of P, since the former were determined first to avoid bias. All the results are consistent within their own errors except possibly the mean-pulse-height estimate, with which one must include an uncertainty based on confusion as to which data channels ought to be included. Qualitative error estimates from the graphical methods are larger than those computed in the numeric methods, but may better take into account difficulties based on the shapes of the distributions which later may give nonlinear effects as a function of energy. The least-squares solutions for P seem stable as the channel range is varied, and the single iteration one-parameter refinement by hand gave the same results as the full machine procedure, starting from good estimates based on any of the graphical methods. There is considerable experience to support the above conclusions in typical cases other than the data of Fig. 3 (Co61).

B. Establishing the Energy vs Pulse-Height Relationship

Once peak positions and uncertainties $(P_i \pm \rho_i)$ have been determined

for all important full-energy peaks in the experimental spectra, an energy scale for pulse height may be established if drifts have been compensated for or shown to be small by the methods described in Sect. IV.C.2. Drift corrections are hazardous if larger than the quoted uncertainties in the peak positions, so one must often seek a more consistent set of data.

Interpolation methods of two types will be discussed. The first employs only two calibration points and assumes local or tangential linearity, perhaps after a linearization technique has already been employed. The second uses in a weighted least squares procedure all the data available over the energy region of interest, and may employ terms nonlinear in the energy.

1. The Two-Point Interpolation Method. -- Suppose that $E \pm \epsilon$ are the unknown energy and standard error for a peak at position $P \pm \rho$ and suppose that calibration at energies $E_1 \pm \epsilon_1$ and $E_2 \pm \epsilon_2$ yielded peaks at $P_1 \pm \rho_1$ and $P_2 \pm \rho_2$. It is assumed that the pulse-height vs energy relation is linear over this region or that it has been adequately linearized. Let

$$f_1 = (P - P_1)/(P_2 - P_1) \text{ and } f_2 = 1 - f_1 \quad . \tag{20}$$

Then

$$E = f_2 E_1 + f_1 E_2 \quad , \tag{21}$$

and

$$\epsilon^2 = f_2^2\, \epsilon_1^2 + f_1^2\, \epsilon_2^2 + g^2\, (\rho^2 + f_2^2\, \rho_1^2 + f_1^2\, \rho_2^2) \tag{22}$$

if the conversion gain $g \cong (E_2 - E_1)/(P_2 - P_1)$. The expression for ϵ^2 assumes that all the errors are uncorrelated, so any estimated systematic component of the ρ's should be combined more carefully.

These relations may be used for short-range extrapolations outside the interval (P_1, P_2), though estimated errors become larger because

one of the f's will have magnitude greater than unity. The two-point calibration method throws away any available information from distant calibration points, but in return is not concerned about the form of the nonlinearities which most likely exist over the more extended pulse-height range. Since fewer output parameters are required, the reduced amount of utilized input data is of less concern than might be thought. When only two calibration points are so used there is no redundant information to illuminate mistakes; therefore extra care is required.

2. A Weighted Least-Squares Interpolation Method. -- It is assumed below that a set of a few parameters is desired to represent the I data couplets (E_i, P_i). The resulting interpolation formula is expected to resemble a straight line and to be linear in the parameters b_σ. From the discussion of peak-fitting procedures above it follows that the latter condition may be removed at the price of an iterative procedure to obtain the solution.

We assume that no output information is desired concerning the most consistent values of the E_i, as would be available from the least-squares calibration method described by Julke et al. (Ju62). If it should be necessary to use as calibration standards any gamma rays having energy values whose relative uncertainty ϵ_j/E_j is comparable to the relative pulse-height uncertainty ρ_j/P_j, we plan to reduce accordingly the weight of the ith observation.

We seek a relation to approximate P_i vs E_i of the form

$$P_i = \sum_{\sigma}' b_\sigma F_{i\sigma} \qquad (23)$$

for all i. Here the b_σ are the desired parameters and $F_{i\sigma}$ are the values of some functions $f_\sigma(E)$ at $E = E_i$. For example, if a simple quadratic expression is sought,

$$P_i \cong b_1 + b_2 E_i + b_3 E_1^2 \quad , \qquad (24)$$

$F_{i1} = 1$ and $F_{i2} = E_i$ for each data point.

It is proposed to find the values of the b_σ by minimizing S, the weighted sum of squared residuals between the experimental data and the interpolated values:

$$S = \sum_i W_i (P_i - \sum_\sigma b_\sigma F_{i\sigma})^2 = (\underline{P} - \underline{Fb})^T \underline{W} (\underline{P} - \underline{Fb}) \quad . \tag{25}$$

The summation form for S as given above assumes that the P_i's are uncorrelated, while the vector notation is more general but reduces to the summation form in the case of no correlation. In the vector notation, which is used below for compactness, $\underline{P}$ and $\underline{b}$ are column vectors, T signifies the transpose, $\underline{F}$ is a I × Σ matrix, where Σ is the number of parameters, and $\underline{W}$ is an I × I matrix which must be diagonal to reproduce the summation form in Eq. (25).

The well-known solution is*

$$\underline{b} = \underline{Q}^{-1} \underline{F}^T \underline{W} \underline{P} \quad , \tag{26}$$

with a parameter variance matrix, based on input errors, of $\underline{V}(\underline{b}) = \underline{Q}^{-1}$, where the least-squares matrix $\underline{Q} = \underline{F}^T \underline{W} \underline{F}$ is assumed to have an inverse. Practical use of Eq. (25) depends on overcoming the following problems:

a. "Best" values of E_i and P_i must be chosen.

b. Based on uncertainties in these quantities a weighting matrix $\underline{W}$ must be formed.

---

*For a two-parameter fit to determine b_1 and b_2 in an approximation of the linear form $P_i \cong b_1 + b_2 E_i$, Eq. (26) expands to

$$b_1 = \left[\left(\sum W_i P_i \right) \left(\sum W_i E_i^2 \right) - \left(\sum W_i P_i E_i \right) \left(\sum W_i E_i \right) \right] / D \quad ,$$

and

$$b_2 = \left[- \left(\sum W_i P_i \right) \left(\sum W_i E_i \right) + \left(\sum W_i P_i E_i \right) \left(\sum W_i \right) \right] / D \quad ,$$

where the determinant $D = \left(\sum W_i E_i^2 \right) \left(\sum W_i \right) - \left(\sum W_i E_i \right)^2$.

c. A functional form $f(E_i; \underline{b})$ must be chosen. It must fit the observed data and lead to sensible interpolated values.

d. A method must be found to extract from $f(E; \underline{b})$ the energy and uncertainty for an unknown energy E given the corresponding peak position $P \pm \rho$.

Problems a and b have been discussed in the early part of this section, but a prescription must still be given below for the formation of $\underline{W}$. Item c can generally be resolved by a function very close to a straight line, especially if linearization techniques have been used. In such a case there is little danger of nonphysical interpolated values. Finding the E for a given P is trivial for the strictly linear case, but might involve iterative techniques if the experimenter is forced to choose an unfavorable form for $f(E; \underline{b})$. We treat later the determination of a standard error for E.

Forming the weight matrix is not formidable in the assumed case of uncorrelated input data, since only the diagonal elements W_{ii} are non-zero, one to represent the weight of each data point. It can be shown (Sc59) that if only the errors in the P_i are significant the minimum variance result is obtained with $W_i = 1/\rho_i^2$. This should be the standard procedure whenever the estimated relative error of the calibration energy is small compared with that of the peak position. This condition is met with well-established calibration lines such as ^{203}Hg or ^{137}Cs or annihilation radiation, but is in jeopardy if more poorly known sources must be employed. A reasonable procedure, followed by the authors, is to use the weight given by

$$1/W_{ii} = \rho_i^2 + \left(\frac{\partial f}{\partial E_i} \right)^2 \epsilon_i^2 \quad , \tag{27}$$

where $\frac{\partial f}{\partial E_i}$ is just the slope of the P vs E relation in the neighborhood of E_i. This relation performs the necessary de-weighting in the case that E_i is poorly known, but we have not shown that it leads to parameters or interpolated values having minimum variance for the given data set except in the case of a one-parameter fit. Use of the weight of

Eq. (27) gives the same result, after analysis, as the bivariate least-squares treatment of Deming (De44), which recognizes at its outset uncertainties in both coordinates of experimental data.

A word is necessary concerning the proper introduction of estimated systematic errors into the system. When such errors seem to be uncorrelated from one point to the next, they may be incorporated into the ρ_i. However, if the systematic uncertainty affects all the P_i in a similar manner,* it should not be included prior to the formation of a diagonal weighting matrix.** After the interpolation for the unknown energy has been completed, the estimated effect of the systematic uncertainty on the final answers should be included in the final error estimate. If this rule of procedure is not followed, reasonable ρ_i can lead to quite unreasonably small error estimates for interpolated values.

Errors in the final interpolated energies may be based on the input errors ρ_i in P_i and perhaps significant errors ϵ_i in some of the calibration energies E_i. We have available the output (previously) unknown energy E gained from the final implicit relationship $P = f(E; \underline{b}) = \sum_\sigma b_\sigma f_\sigma(E)$. The parameters b_σ are also known, along with an estimate of the parameter variance matrix*** $\underline{V}(\underline{b}) = \underline{Q}^{-1} = [\underline{F}^T \underline{W} \underline{F}]^{-1}$.

*One example might be a possible gain or zero drift between calibration data and measurement of the spectrum from the unknown.

**Such a case can be handled using a nondiagonal weighting matrix with little additional labor, provided that the computations are being performed by machine. In all simple cases which have been considered, the results are equivalent to the recommended procedure. However, the nondiagonal weighting allows for great flexibility in handling estimable systematic errors which affect only certain parts of the data. In this general case the weight matrix is taken as the inverse of the variance matrix of the input data.

***This estimate depends wholly upon the weighting matrix $\underline{W}$ for its information, so it assumes that $f(E; \underline{b})$ properly fits the input data within the errors ρ_i used in forming $\underline{W}$. A partially defensible and popular approach is to test the ratio $"\chi^2/\nu" = S/(I - \Sigma)$, which should be about unity if the degree of fit is consonant with estimated errors, and use $\underline{V}'(\underline{b}) = S\,\underline{Q}^{-1}/(I - \Sigma)$ instead of $\underline{V}(\underline{b})$ as given above. S is from Eq. (25). This method assumes that the relative weights assigned to the data points are appropriate but that all the errors should be increased by a fixed scaling factor. If input errors have been estimated carefully, it is unlikely that $\underline{V}'$ should be used when it is smaller than $\underline{V}$.

The estimated standard errors in the fitting parameters b_σ are just the square root of the diagonal elements of $\underline{V}(\underline{b})$. However, since the parameters are heavily correlated, the off-diagonal terms must be considered to obtain a reasonable estimate for the error ϵ in the unknown energy E. This would be a simple problem if the solution for E were not buried in the implicit relation $P = f(E; \underline{b})$.

In any case one must form, by numerical means if necessary, the partial derivatives $\partial E/\partial P$ and $h_\sigma \equiv \partial E/\partial b_\sigma$ for all σ. This requirement implies a calculational advantage if the functional form for f is easily solved for E. One then has

$$\epsilon^2 = (\partial E/\partial P)^2 \rho^2 + \underline{h}^t \underline{V}(\underline{b}) \underline{h} \qquad (28)$$

if the error ρ in P is independent of the errors in the parameters. If there were several unknown energies E_k, the above treatment could be cast in matrix notation for easy handling. In this case, one obtains a variance matrix which expresses the errors in all the output energies as well as what are likely to be important correlations between them. These correlations are significant if the output energy values from one experiment are to be used as input data for further data analysis, just as the off-diagonal terms in $\underline{V}(\underline{b})$ are important in Eq. (28).

VI. CONCLUSION

This report has dealt in detail with methods for analyzing energy calibration data, but we suggest that obtaining high-quality experimental results is the difficult task which confronts the scintillation spectrometrist. The authors contemplate below a salient class of measurements and inventions which, if accomplished, could lead to improved accuracy, with less difficulty both in the laboratory and at the computer. The order does not connote priority.

A. Additional Standard Sources

Error limits much less than 0.1% are evidently difficult to attain by any gamma-spectrometric method. At the present, too few gamma rays

have been determined by diffraction or magnetic methods for the scintillation spectroscopist who requires standards having well-isolated lines. Standards are badly needed in some energy ranges, as evidenced by the low precision to which many of the most useful standard energies are known (see Ro63, and Table 1 in Sect. II). Those having suitable equipment should be encouraged to take up this assignment, which lithium-drifted germanium detectors will apparently make practical.

B. NaI(Tl) Response Data

The data available demonstrate conclusively the nonproportional response of NaI(Tl) (see Sect. IV). Even more precise and complete information is required to allow later experimenters to linearize their experimental energy scales. Experimental results in this field should be presented in a manner which eases the derivation of such corrections.

C. A Reliable "Sliding" Pulser

We have indicated in Sect. IV that sliding pulsers would provide a good check of electronic linearity if a design could be found with testable linearity, adequate pulse repetition rate (~500 counts/sec), and appropriate pulse shape. This project deserves more attention from instrumentation experts.

D. A Stable Light Pulser

To make gain stabilization fully practical, a small, convenient, and quite reliable stable light pulser yielding an appropriate pulse shape must be invented for routine inclusion into scintillator assemblies. The light intensity will have to be adjustable over the range of importance to scintillation spectroscopy. It is desired but not essential that the light output be a precisely known function of the operating conditions so that system proportionality curves might be obtained using it as the light source.

E. Comprehensive Gain Stabilizers

Good gain stabilization methods have been discussed in Sect. III,

but a simple one must be devised which includes the multiplier phototube within the stabilized loop. Unless the above-mentioned light pulser (Sect. VI.D.) is realized, the methods of Dudley and Scarpatetti (Du64) and of Hinricksen (Hi64) using tagged pulses from radioactive sources should be developed. If this step could be quite generally accomplished, a shorter section on drifts would appear in the next publication of this type. A statistical analysis is required to indicate whether the error signal ought to be generated from counting rate differences or from accumulated count differences.

F. Premium High-Linearity Low-Drift Pulse-Height Analyzers

If linearity checks and corrections are not always to plague the scintillation spectroscopists, pulse-height analyzers must be produced that are almost an order of magnitude more linear than those now advertized, and less sensitive to changes in input pulse shape. Analyzer stability could more easily be improved beyond any need for concern.

When these innovations are available, each scintillation spectroscopist will be able to relax a little concerning questions of technique and devote more attention to his own discipline.

REFERENCES

Aj59 F. Ajzenberg-Selove and T. Lauritsen, Nucl. Phys. 11, 1, 206 (1959).

Al53 D. E. Alburger, Phys. Rev. 92, 1257 (1953).

Ax54 P. Axel, Rev. Sci. Instr. 25, 391 (1954).

Ba56 G. Backström, Arkiv Fysik 10, 393 (1956).

Ba63 A. A. Bartlett et al., Bull. Am. Phys. Soc. 8, Q8 (1963).

Be55 P. R. Bell, R. C. Davis, and W. Bernstein, Rev. Sci. Instr. 26, 726 (1955).

Be57 J. B. Bellicard and A. Moussa, J. Phys. Radium 18, 115 (1957).

Bi58 A. Bisi and L. Zappa, Nucl. Instr. 3, 17 (1958).

Bo60 I. F. Boekelheide, Rev. Sci. Instr. 31, 1001 (1960).

Br55 E. Breitenberger, Progr. Nucl. Phys. 4, 56 (1955).

Bu62 W. R. Busing and H. A. Levy, A General Fortran Least-Squares Program, Oak Ridge National Laboratory Report ORNL-TM-271, unpublished (1962).

Ca53 K. M. Case, F. de Hoffmann, and G. Placzek, Introduction to the Theory of Neutron Diffusion, Vol. 1, U. S. Govt. Printing Office, Washington (1953).

Ca58 L. Cathey, IRE Trans. Nucl. Sci. NS-5, No. 3, 109 (1958).

Ca61 L. Cathey, Control of Fatigue in Photomultipliers, AEC Research and Development Report DP-642 (1961).

Ca64 I. Cantarell, Nucl. Sci. Eng. 18, 31 (1964).

Ca65 I. Cantarell and I. Almodovar, Intern. J. Appl. Radiation Isotopes 16, 91 (1965).

Ch58 E. L. Chupp et al., Phys. Rev. 109, 2036 (1958).

Ch60 R. Chéry, J. Phys. Rad. 21, 679 (1960).

Ch62 R. L. Chase, IRE Trans. Nucl. Sci. NS-9, 1 (1962).

Ch63 R. O. Chester, R. W. Peelle, and F. C. Maienschein, p. 201 in Applications of Computers to Nuclear and Radiochemistry, edited by G. D. O'Kelley, National Academy of Sciences, National Research Council, NAS-NS-3107 (1963).

Co51 J. M. Cork et al., Phys. Rev. 84, 596 (1951).

Co55 E. R. Cohen et al., Rev. Mod. Phys. 27, 363 (1955).

Co60 R. D. Connor and M. K. Hussain, Nucl. Instr. Methods 6, 337 (1960).

Co61 R. L. Cowperthwaite, University of Tennesse, private communication (1961).

Co61a D. F. Covell and B. A. Euler, Proceedings of the 1961 International Conference on Modern Trends in Activation Analysis, College Station, Texas (1961); Also see USNRDL-TR-521 (1961).

Co63 E. R. Cohen and J. W. M. DuMond, p. 152 in Proceedings Second International Conference on Nucleidic Masses, Vienna, Springer-Verlag (1963).

Cr63 D. F. Crouch and R. L. Heath, Routine Testing and Calibration Procedures for Multichannel Pulse Analyzers and Gamma-Ray Spectrometers, AEC Research and Development Report IDO-16923 (1963).

Da55 G. F. von Dardel, J. Sci. Instr. 32, 306 (1955).

De44 W. E. Deming, Statistical Adjustment of Data, John Wiley, New York (1944).

Di63 I. Dixon, Nucl. Instr. Methods 25, 26 (1963).

Dr59 J. E. Draper and W. J. Alston, Rev. Sci. Instr. 30, 805 (1959).

Du64 R. A. Dudley and R. Scarpatetti, Nucl. Instr. Methods 25, 297 (1964).

Ed58 K. Edvarson, K. Siegbahn, and A. H. Wapstra, communication quoted in G. J. Nigjh et al., Nucl. Phys. 9, 528 (1958).

En52 R. W. Engstrom, R. G. Stoudenheimer, A. M. Glover, Nucleonics 10, No. 4, 58 (1952).

En56 D. Engelkemeir, Rev. Sci. Instr. 27, 589 (1956).

Fa62 E. Fairstein, pp. 244, 259 in Nuclear Instruments and Their Uses, edited by A. H. Snell, John Wiley, New York (1962).

Ha60 S. Hann and D. Kamke, Nucl. Instr. Methods 8, 331 (1960).

He52 A. Hedgran and D. Lind, Arkiv Fysik 5, 177 (1952).

He65 R. L. Heath et al., The Calculation of Gamma-Ray Shapes for Sodium Iodide Scintillation Spectrometers ... Computer Programs and Experimental Problems, AEC Research and Development Report IDO-17017 (1965).

Hi64 P. F. Hinricksen, IRE Trans. Nucl. Sci. NS-11, No. 3, 420 (1964).

Ho53 H. C. Hoyt and J. W. M. DuMond, Phys. Rev. 91, 1027 (1953).

Ir62 P. Iredale, Proceedings of the Conference on Nuclear Electronics, Vol. 1, IAEA, Vienna, p. 87 (1962).

Ja61 L. Jarczyk et al., Nucl. Instr. Methods 13, 287 (1961).

Ju60 H. Jung, P. H. Panussi, and J. Jänecke, Nucl. Instr. Methods 9, 121 (1960).

Ju62 R. T. Julke et al., The Measurement of Energy and Intensity of Gamma Rays by Use of a Scintillation Spectrometer, Argonne National Laboratory Report ANL-6499 (1962).

Ka61 J. Kantele and R. W. Fink, Nucl. Instr. Methods 13, 141 (1961).

Ka62 W. C. Kaiser et al., IRE Trans. Nucl. Sci. NS-9, No. 3, 22 (1962).

Ka65 C. J. Karzmark, Health Physics 11, 54 (1965).

Ke63 Q. A. Kerns and R. F. Tusting, Contant-Amplitude Light-Flash Generator for Gain Stabilization of Photosensitive Systems, University of California Radiation Laboratory Report UCRL-10895 (1963).

Ko64 I. Koosman, IRE Trans. Nucl. Sci. NS-11, No. 3, 56 (1964).

Kr65 H. R. Krall, IRE Trans. Nucl. Sci. NS-12, No. 1, 39 (1965).

La61 J. A. Ladd and J. M. Kennedy, A Digital Spectrum Stabilizer for Pulse Analyzing Systems, Atomic Energy of Canada Limited Report AECL-1417 (1961).

Li53 G. Lindstrom et al., Proc. Phys. Soc. (London) 66B, 54 (1953).

Li54 K. Liden and N. Starfelt, Arkiv Fysik 7, 427 (1954).

Ma47 F. Marshall, J. W. Coltman, and L. P. Hunter, Rev. Sci. Instr. 18, 504 (1947).

Ma62 W. W. Managan, IRE Trans. Nucl. Sci. NS-9, 1 (1962).

Ma62a K. W. Marlow, Nucl. Instr. Methods 15, 288 (1962).

Ma63 I. Marklund and B. Lindström, Nucl. Phys. 40, 329 (1963).

Mc65 J. W. McConnel, Nanosecond Light Sources for Gain Stabilization, Oak Ridge National Laboratory Report ORNL-TM-985 (1965).

Mi52 W. E. Millet, Effects of Longitudial Magnetic Field on the Resolution of a 5819-NaI Scintillation Spectrometer, Oak Ridge National Laboratory Report ORNL-1335 (1952).

Mo58 W. E. Mott and R. B. Sutton, p. 131 in Handbuch der Physik, Vol. 45, edited by S. Flügge, Springer, Berlin (1958).

Mo61 J. E. Monahan, S. Raboy, and C. C. Trail, Phys. Rev. 123, 1373 (1961).

Mu52 D. E. Müller et al., Phys. Rev. 88, 775 (1952).

Mu60 R. B. Murray and J. J. Manning, IRE Trans. Nucl. Sci. NS-7, No. 2-3, 80 (1960).

Mu61 R. B. Murray and A. Meyer, Phys. Rev. 122, 815 (1961).

Mu63 G. Murray, R. L. Graham, and J. S. Geiger, Nucl. Phys. 45, 177 (1963).

Mu65 G. Murray, R. L. Graham, and J. S. Geiger, Nucl. Phys. 63, 353 (1965).

Na65 M. Nakamura and R. L. LaPierre, Nucl. Instr. Methods 32, 277 (1965).

No61 R. Nordhagen, Nucl. Instr. Methods 12, 291 (1961).

Nu65 Nuclear Data Sheets, National Academy of Sciences, National Research Council, NAS-NRS, through February 1965.

Pe60 R. W. Peelle and T. A. Love, Rev. Sci. Instr. 31, 205 (1960).

Pe60a R. W. Peelle and T. A. Love, Scintillation Spectroscopy Measurements of Gamma-Ray Energies from Sources of ^{88}Y, ^{54}Mn, and ^{65}Zn,, Oak Ridge National Laboratory Report ORNL-2790 (1960).

Pu65 M. Putnam et al., A Nonlinear Least-Square Program for the Determination of Parameters of Photopeaks by the Use of a Modified-Gaussian Function, AEC Research and Development Report IDO-17016 (1965).

Rc63 RCA Technical Manual, PT-60, Harrison, New Jersey (1963).

Ri61 H. J. Rijks, Nucl. Instr. Methods 14, 76 (1961).

Ro63 B. L. Robinson, p. 72 in Applications of Computers to Nuclear and Radiochemistry, edited by G. D. O'Kelley, National Academy of Sciences, National Research Council, NAS-NS-3107 (1963).

Ro63a B. L. Robinson, Western Reserve University, private communication (1963).

Ro65 R. L. Robinson et al., Nucl. Phys. 74, 281 (1965).

Ro65a R. E. Rohde, Nucl. Instr. Methods 34, 109 (1965).

Sa58 A. E. Sandström, pp. 226-37 in Handbuch der Physik, Vol. 30, edited by S. Flügge, Springer, Berlin (1958).

Sc56 W. Van Sciver, IRE Trans. Nucl. Sci. NS-3, No. 4, 39 (1956). (Quoted in Mo58, p. 98.)

Sc59 H. Scheffe, p. 19 in The Analysis of Variance, John Wiley, New York (1959).

Sh64 I. S. Sherman, IRE Trans. Nucl. Sci. NS-11, No. 3, 20 (1964).

St58 D. Strominger, J. M. Hollander, and G. T. Seaborg, Rev. Mod. Phys. 30, 826 (1958).

St60 V. I. Startsev, Z. B. Baturichera, and V. A. Tsirlin, Opt. Spectry. (USSR) 8, No. 4, 286 (1960).

St64 F. Stenman, Nucl. Instr. Methods 29, 107 (1964).

Va61 F. P. G. Valckx, Nucl. Instr. Methods 10, 234 (1961).

Wa55 H. de Waard, Nucleonics 13, No. 7, 36 (1955).

Wa59 A. H. Wapstra, G. J. Nijgh, and R. Van Lieshout, pp. 76-87 in Nuclear Spectroscopy Tables, North Holland Publishing Co., Amsterdam (1959).

Wi50 D. H. Wilkinson, J. Sci. Instr. 27, 36 (1950).

Wo65 J. Woody, Oak Ridge National Laboratory, private communication (1965).

Ya55 A. I. Yavin and F. H. Schmidt, Phys. Rev. 100, 171 (1955).

Ze59 C. Zerby and H. Moran, Bremsstrahlung Spectra in an Infinite NaI Crystal, Oak Ridge National Laboratory Report ORNL-2754 (1959).

Ze61 C. D. Zerby, A. Meyer, and R. B. Murray, Nucl. Instr. Methods 12, 115 (1961).

Zi61 W. Zimmerman, Rev. Sci. Instr. 32, 1063 (1961).

ORNL-4118
UC-34 — Physics

INTERNAL DISTRIBUTION

1. Biology Library
2-4. Central Research Library
5-6. ORNL — Y-12 Technical Library Document Reference Section
7-221. Laboratory Records Department
222. Laboratory Records, ORNL R.C.
223. L. S. Abbott
224. J. K. Bair
225. L. C. Bate
226. C. D. Baumann
227. R. D. Birkhoff
228. J. L. Blankenship
229. H. R. Brashear
230. V. R. Cain
231. R. M. Carroll
232. M. M. Chiles
233. W. T. Clay
234. C. E. Clifford
235. E. Cofield
236. J. K. Dickens
237. J. S. Eldridge
238. R. L. Ferguson
239. R. M. Freestone, Jr.
240. J. Halperin
241. L. B. Holland
242. H. H. Hubbell
243. G. S. Hurst
244. R. W. Ingle
245. W. H. Jordan
246. C. E. Larson
247. T. A. Love
248. J. L. Lovvorn
249. W. S. Lyon
250. H. G. MacPherson
251. R. E. Maerker
252. D. W. Magnuson
253. F. C. Maienschein
254. V. A. McKay
255. F. K. McGowan
256. M. T. Morgan
257. F. J. Muckenthaler
258. C. W. Nestor, Jr.
259. J. P. Nichols
260. J. Olson
261. G. D. O'Kelley
262. B. H. Kettelle
263. R. W. Peelle
264. J. K. Poggenburg
265. J. W. Reynolds
266. R. T. Santoro
267. R. L. Shipp
268. O. Sisman
269. M. J. Skinner
270. J. E. Strain
271. E. Straker
272. J. R. Tarrant
273. D. R. Vondy
274. A. M. Weinberg
275. G. Dessauer (consultant)
276. B. C. Diven (consultant)
277. W. N. Hess (consultant)
278. M. H. Kalos (consultant)
279. L. V. Spencer (consultant)

EXTERNAL DISTRIBUTION

280. P. B. Hemmig. Division of Reactor Development and Technology, U.S. Atomic Energy Commission, Washington, D.C. 20545
281. I. F. Zartman, Division of Reactor Development, U.S. Atomic Energy Commission, Washington, D.C. 20545
282. J. A. Swartout, Union Carbide Corporation, New York
283. Laboratory and University Division, AEC, ORO
284-572. Given distribution as shown in TID-4500 under Physics category